A role for JAK2 in mediating cell surface GHR-PRLR interaction

Chen Chen[1,2], Jing Jiang[2], Tejeshwar C. Rao[3,4], Ying Liu[2,5], Tatiana T. Marquez Lago[1], Stuart J. Frank[*2,3], André Leier[*1,3]

[1]Department of Genetics, Heersink School of Medicine, University of Alabama at Birmingham, Birmingham, USA
[2]Division of Endocrinology, Diabetes, and Metabolism, Department of Medicine, Heersink School of Medicine, University of Alabama at Birmingham, Birmingham, USA
[3]Department of Cell, Developmental, and Integrative Biology, Heersink School of Medicine, University of Alabama at Birmingham, Birmingham, USA
[4]Department of Pharmacological and Pharmaceutical Sciences, University of Houston, Houston, USA
[5]Division of Hematology and Oncology, Department of Medicine, NYU Grossman School of Medicine, New York University, New York, USA

[*]Co-corresponding authors

Abstract

Growth hormone (GH) receptor (GHR) and (full-length) prolactin (PRL) receptor (PRLR) are transmembrane class I cytokine receptors that co-exist in various normal and cancerous cells. Both receptors respond to their associated ligands predominantly by activating the Janus Kinase 2 (JAK2)-signal transducer and activator of transcription (STAT) signaling pathways, and both are also known to initiate receptor-specific JAK2-independent signaling. Together with their cognate ligands, these receptors have been associated with pro-tumorigenic effects in various cancers, including breast cancer (BC). Human GH is known to bind GHR and PRLR, while PRL can only bind PRLR. A growing body of work suggests that GHR and PRLR can form heteromers in BC cells, modulating GH signal transduction. However, the dynamics of PRLR and GHR on the plasma membrane and how these could affect their respective signaling still need to be understood.

To this end, we set out to unravel the spatiotemporal dynamics of GHR and PRLR on the surface of human T47D breast cancer cells and γ2A-JAK2 cells. We applied direct stochastic optical reconstruction microscopy (dSTORM) and quantified the colocalization and availability of both receptors on the plasma membrane at the nanometer scale at different time points following treatment with GH and PRL. In cells co-expressing GHR and PRLR, we surprisingly observed that not only GH but also PRL treatment induces a significant loss of surface GHR. In cells lacking PRLR or expressing a mutant PRLR deficient in JAK2 binding, we observed that GH induces downregulation of cell surface membrane-bound GHR, but PRL no longer induces loss of surface GHR. Colocalizations of GHR and PRLR were confirmed by proximity ligation (PL) assay.

Our results suggest that PRLR-GHR interaction, direct or indirect, is indispensable for PRL- but not GH-induced loss of surface GHR and for both GH-induced and PRL-induced increase of surface PRLR, with potential consequences for downstream signaling. Furthermore, our results suggest that JAK2 binding via the receptor intracellular domain's Box1 element is crucial for the observed regulation of one class I cytokine receptor's cell surface availability via ligand-induced activation of another class I cytokine

receptor. Our findings shed new light on the reciprocal and collective role that PRLR and GHR play in regulating cell signaling.

Keywords: growth hormone receptor, prolactin receptor, Box1, JAK2, super-resolution microscopy, direct stochastic optical reconstruction microscopy (dSTORM)

Introduction

Growth hormone (GH) and prolactin (PRL) are hormones emanating mainly from the anterior pituitary. The primary function of GH is regulating anabolism and metabolism [1, 2], while PRL has important roles in breast development and lactation [3]. There is mounting evidence pointing at both hormones and their receptors playing roles in various types of cancer [4-11], including breast cancer (BC) [12-17], where GHR is frequently present and PRLR is often found overexpressed [18-25]. While they have been mostly associated with pro-tumorigenic effects, PRL has also been reported to show anti-tumor effects and, like PRLR, has been associated with good prognosis in certain BC subtypes [26-29]. However, a humanized neutralizing monoclonal antibody directed against the extracellular domain of PRLR showed no anti-tumor effect when administered in patients with PRLR-positive metastatic BC [30]. This suggests that PRLRs' pro-tumorigenic function may not be as relevant as previously thought or depends on other circumstances such as the presence or absence of other hormone receptors, with which they may interact.

Both GH receptor (GHR) and PRL receptor (PRLR) are structurally similar transmembrane glycoproteins and belong to the class I cytokine receptor superfamily [31, 32]. As is characteristic of the majority of their superfamily members, both receptors contain a proline-rich Box1 motif in the membrane-proximal region of their intracellular domains (ICDs), which is followed by a short inter-box region, and a less conserved Box2 motif that is rich in acidic and aromatic residues [33-35]. For both receptors different isoforms have been identified: GHR has three additional isoforms two of which are created through alternative splicing events and lack the Box1-Box2 motif [36] and the third is the exon 3 deleted GHR (d3-GHR). Aside from the PRLR long (or full length) isoform (LF), other membrane-bound isoforms have been identified, including a long form lacking domain D1 (ΔS1), an intermediate form (IF), and the short forms S1a, S1b, and S1c [3, 37]. All isoforms except for S1b and S1c contain the Box1-Box2 motif, but S1b and S1c still contain the Box1 motif. If not specifically stated otherwise, we will refer here by default to the receptors' full-length (or long) isoforms.

GH can bind and introduce a conformational change to both GHR and PRLR, allowing receptor activation and downstream signaling [38-42], but, unlike GH, PRL can only bind to PRLR [41, 43-45]. Both GHR and PRLR lack intrinsic kinase activity. Following ligand binding, downstream signal transduction involves predominantly activating the associated cytoplasmic tyrosine kinase, Janus kinase 2 (JAK2), bound to the receptors' Box1 elements. This is followed by phosphorylation of the signal transducer and activator of transcription 5 (STAT5a and STAT5b) [46, 47], although other receptor-specific JAK2-independent signal transduction pathways may also be activated. Of note, JAK2 is not only activating the canonical JAK2-STAT5 pathway, but it can also signal via STAT1 and STAT3 [48-51] and activate non-canonical kinase pathways such as Ras/Raf/MAPK/ERK [52-54] and PI3K/Akt/mTOR [55-58], as well as influence gene expression through histone modification [59, 60]. Moreover, activation of PRLR downstream pathways is isoform-specific, with the short isoforms activating the MAPK and PI3K pathways [61-63]. For comprehensive reviews of JAK2-independent signaling pathways, we refer the reader to [64, 65].

Increasing evidence indicates that GHR and PRLR interact. Two decades ago, it was shown that ovine GHR (oGHR) and PRLR (oPRLR) can tightly associate with each other following stimulation with placental lactogen [66]. These studies utilized chimeric receptors consisting of the extracellular domain (ECD) of human granulocyte and macrophage colony-stimulating factor (hGM-CSF) receptor (hGM-CSFR) along with a part of either oGHR ICD or oPRLR ICD. After hGM-CSF treatment of cells co-expressing oGHR chimera and oPRLR chimera, JAK2 was effectively activated, and protein-protein interaction of both

chimeric receptors was detected via co-immunoprecipitation [66, 67]. Additionally, our previous work revealed a specific ligand-independent human GHR (hGHR) - human PRLR (hPRLR) association in human T47D breast cancer cells, which endogenously express both receptors [68]. Further, the use of split luciferase complementation assays has suggested that hGHR homodimers and hPRLR homodimers form hGHR/hPRLR multimers [69] and extracellular subdomain 2 of the hGHR or hPRLR determines the dimerization partner [70]. Although biochemical studies and luciferase complementation assays strongly support the notion that an interplay between hGHR and hPRLR exists, the observed outcomes are ascribed to total receptors within cells, irrespective of subcellular localization.

In the present study, we directly visualized the cell surface interaction of hGHR and hPRLR and how it changes upon ligand treatment. Specifically, we used direct stochastic optical reconstruction microscopy (dSTORM) [71] to visualize single receptor clusters of hGHR and hPRLR on cell surfaces. In dSTORM, a super-resolution microscopy technique, individual fluorophores cycle through reversible transitions between a dark and a fluorescent state [72]. Thus, a fluorophore emits photons multiple times before permanently being photobleached. These blinking events and their localizations are recorded and, although the exact number of proteins in clusters is difficult to determine, the number of localizations is strongly correlated with the number of receptors [73, 74]. Thus, the dSTORM approach can deliver high-resolution images to reveal the localization or arrangement of individual membrane receptor systems providing valuable insight into their interactions with other proteins at the cell surface. Given that receptors are highly trafficked to and from the cell surface and to avoid signal detection from cytosolic receptors, we used monoclonal antibodies to distinctly label the extracellular S2 domain of GHR and PRLR on non-permeabilized cells. Descriptive spatial analysis using Ripley's K- and L-function [75] indicates that both hGHR and hPRLR are organized in nanometer-scale clusters on the T47D cell surface. To further gain quantitative information about GHR and PRLR nanoclusters, we applied DBSCAN (density-based spatial clustering of applications with noise) [76]. Subsequently, individual cluster contours were delineated, individual clusters were assigned a cluster ID, and receptor abundance was analyzed separately for each cluster and receptor. By doing so, we detected and calculated homomeric and heteromeric hGHR and hPRLR clusters on cell surfaces. Colocalizations of GHR and PRLR were also confirmed by proximity ligation (PL) assay. Lastly, we explored which receptor domains determine the interaction of hGHR and hPRLR by creating different truncated or modified hPRLR variants. Our findings indicate that the intracellular Box1 region is an essential determinant of hGHR and hPRLR association, suggesting JAK2 may play an important role in the observed ligand-induced and PRLR-mediated downregulation of cell surface GHR – which could also elicit or add to PRLR's observed anti-tumor effect.

Results

Ligands induce an increase in PRLR localizations and a decrease in GHR localizations at the surface of T47D cells

To investigate the dynamic spatial distribution of endogenous hGHR and hPRLR on the surface of breast cancer cells, we used dSTORM under the total internal reflection fluorescence (TIRF) illumination mode [77]. The dSTORM images show that hGHR and hPRLR form nanometer-scale clusters and are broadly distributed on the surface of T47D cells (Fig. 1). To assess the ligands' effects on the spatial distribution of hGHR and hPRLR on the cell surface, we conducted time-course experiments using T47D cells with human GH or human PRL (500 ng/ml each). Such stimulation is known to induce rapid and substantial STAT5

127 phosphorylation [68]. We first analyzed the cell surface localization density (number of localizations per
128 μm^2) of hGHR or hPRLR in both resting and ligand-stimulated conditions. The abundance of surface-hPRLR
129 was rapidly increased, reaching its maximum after 3 min of GH or PRL treatment with a ~5.6-fold and ~4.5-
130 fold increase compared to the basal value, respectively (Fig. 2A and 2B). This increase was followed by a
131 rapid decline: after GH treatment for 5 min, the localization density dropped from 200.6 ± 14.7 per μm^2
132 to 57.2 ± 3.6 per μm^2; after PRL treatment for 5 min, the density fell from 159.4 ± 16.2 per μm^2 to 94.8 ±
133 16.0 per μm^2. In contrast to hPRLR, the density of hGHR significantly decreased from 43.3 ± 5.5 per μm^2
134 basally to 25.8 ± 2.7 per μm^2 after 3min of GH stimulation. After 5 min and 10 min of GH stimulation, the
135 density of hGHR remained relatively low at 26.6 ± 2.3 per μm^2 and 19.3 ± 1.5 per μm^2, respectively (Fig.
136 2C). Surprisingly, PRL, which does not bind to hGHR, also induced a loss of surface hGHR on T47D cells.
137 After 1 min of PRL treatment, only 36% of hGHR remained on the cell surface compared to the basal state,
138 and hGHR density remained low for at least 10 min (Fig. 2D). A schematic illustration of GH- and PRL-
139 induced hGHR and hPRLR density changes is shown in Fig. 2E. We previously observed that hGHR and
140 hPRLR specifically co-immunoprecipitate in the absence of added ligands in T47D cells [68]; thus, we
141 postulate that the propensity of hGHR and hPRLR to physically interact underlies our observed loss of
142 hGHR in response to PRL stimulation.

143

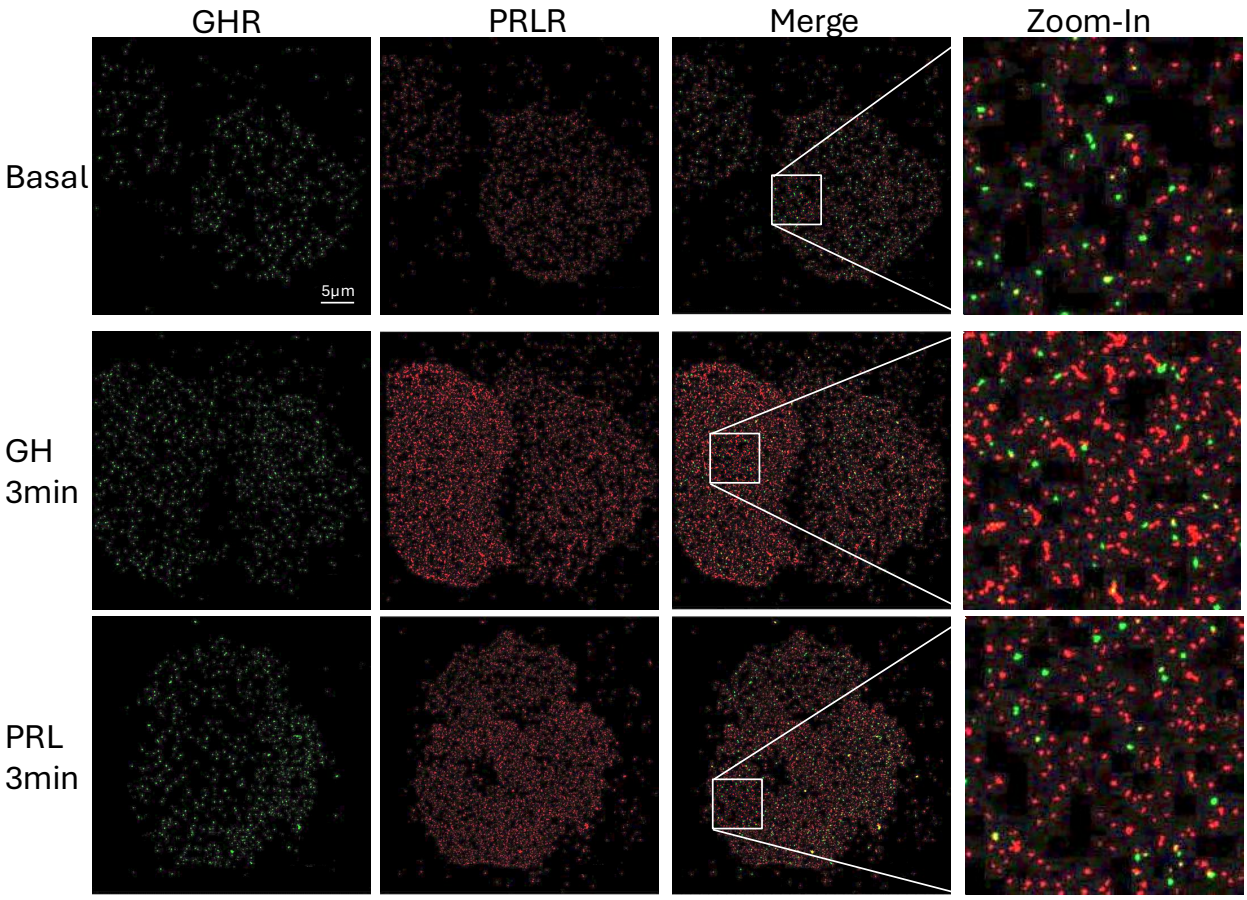

Fig. 1. Ligand-induced increase of PRLR localizations and decrease of GHR localizations at the surface of T47D cells. A representative set of reconstructed dSTORM images, showing Gaussian-fitted localizations obtained from fluorophore blinking events. GHR is labeled with Alexa 568-conjugated antibody (green, channel 1), and PRLR is labeled with Alexa 647-conjugated antibody (red, channel 2). The last column of images shows the merging of these two channels. T47D cells were either left untreated (upper row), exposed to 500ng/mL GH for 3 min (middle row), or exposed to 500ng/mL PRL for 3 min (lower row). Brightness was increased by 40% and Contrast was reduced by 40% to increase visibility. The images in the first three columns (GHR, PRLR, Merge) have the same scale. The scale bar (5µm) is shown in the upper left image. The images in the right most column are zoomed-in sections from the corresponding merged images.

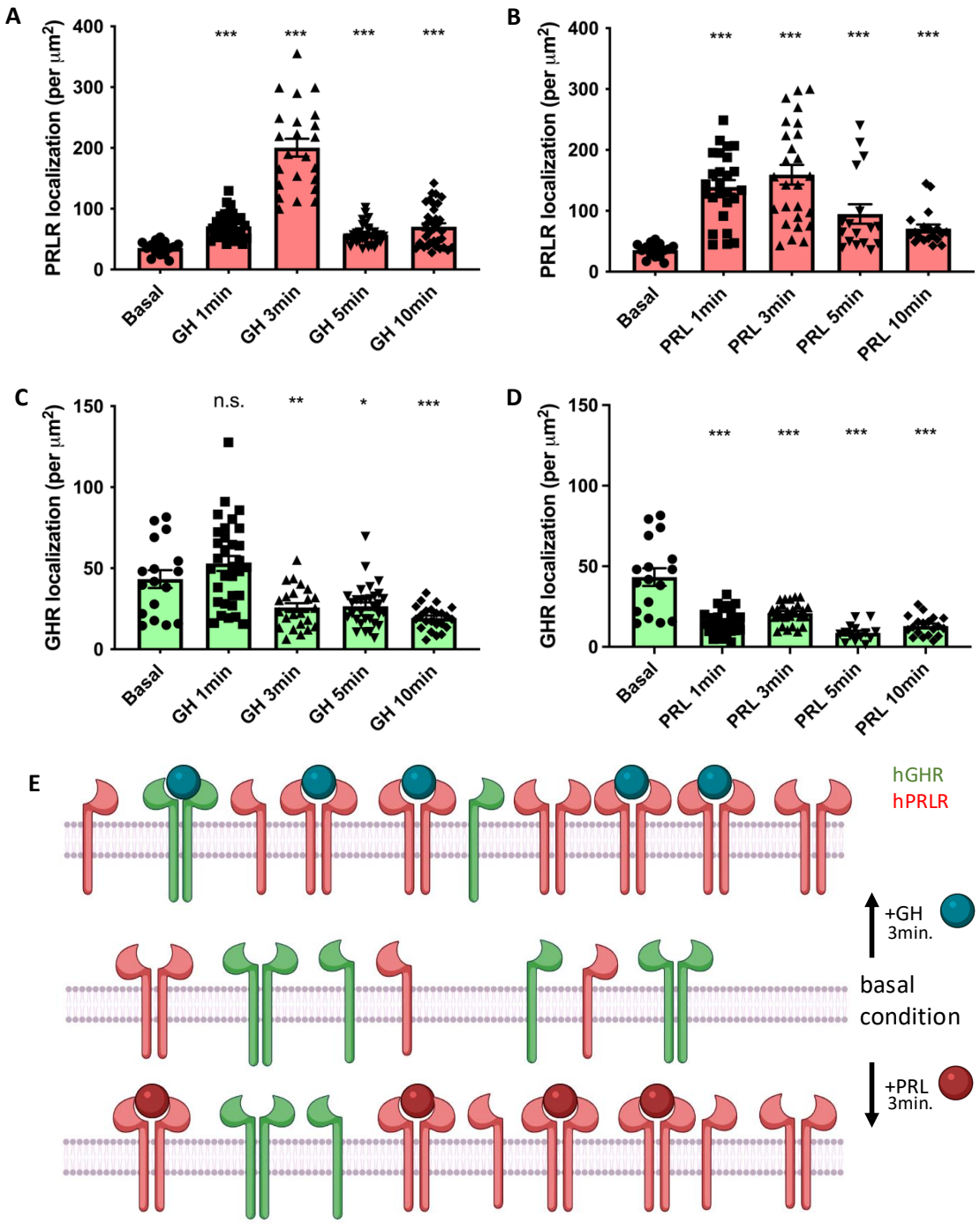

157 **Fig. 2. (A, B)** Quantification of GH-induced (500 ng/ml) (A) and PRL-induced (500 ng/ml) (B) changes of
158 PRLR localizations on the cell surface. **(C, D)** Quantification of GH-induced (C) and PRL-induced (D) changes
159 of GHR localizations on the cell surface. Each data point represents the density of receptors in a 6.25 µm
160 X 6.25 µm area. Data are collected from at least 6 cells from each group and displayed as mean ± SE. *
161 (P<0.05), ** (P<0.01), and *** (P<0.001) indicate the statistical significance in comparison with Basal and
162 are calculated by two-tailed t-tests assuming unequal variances. **(E)** Model depicting hPRLR and hGHR
163 densities and activation schemes in T47D cells. The middle of the three states depicts the basal condition.

GH or PRL stimulation induces a redistribution of hGHR and hPRLR clusters

We analyzed the dSTORM images using the DBSCAN algorithm to identify different clusters and determine the number of receptor localizations within a cluster (termed 'cluster size') (Fig. 3A). We then performed a localization distribution analysis and plotted a histogram of the relative frequency of localizations (termed 'distribution plot' in this study). Representative dSTORM images of hGHR as well as associated distribution plots are shown in Fig. 3B.

To gain a better understanding of the changes in GHR-PRLR colocalizations, we obtained and analyzed the corresponding bivariate cluster size distributions. Their median values are summarized in Fig. 3C and 3D. As can be seen, hGHR responds quickly and transiently to GH stimulation by forming larger clusters. After GH treatment for 1 min, the median number of hGHR blinking events in a cluster reaches its peak and amounts to 85.6 ± 20.9 localizations in comparison with 33.3 ± 1.7 localizations per cluster in the basal state (P value = 0.0035). After 5 min, this number is reduced approximately to its pre-stimulation value (29.1 ± 2.2) but appears to continue to fluctuate for at least another 25 minutes (Fig. 3C). In turn, hPRLR responds to GH in a less prominent manner: The median number of hPRLR blinking events in a cluster in the basal state is 16.5 ± 0.7. After 3 min of GH stimulation, the median of PRLR cluster size reaches its maximum, which is 22.5 ± 3.9 (P value = 0.1496), and afterward declines to its basal level (Fig. 3C).

Like the response to GH, hGHR reacts also quickly to PRL treatment. The median number of hGHR blinking events in a cluster culminates at 1 min of PRL treatment with 45.8 ± 5.0 (compared with basal level, P value = 0.0098). In distinction, hPRLR response to PRL is slower. The median number of hPRLR blinking events in a cluster reaches its peak at 5 min of PRL treatment with a median number of 23.3 ± 2.8 (compared with basal level, P value = 0.0233), and after 10 min the median is only slightly less than that maximum (Fig. 3D). Together, these results indicate that upon ligand stimulation hGHR cluster sizes increase transiently and significantly, while changes of hPRLR cluster sizes occur slowly and more subtly.

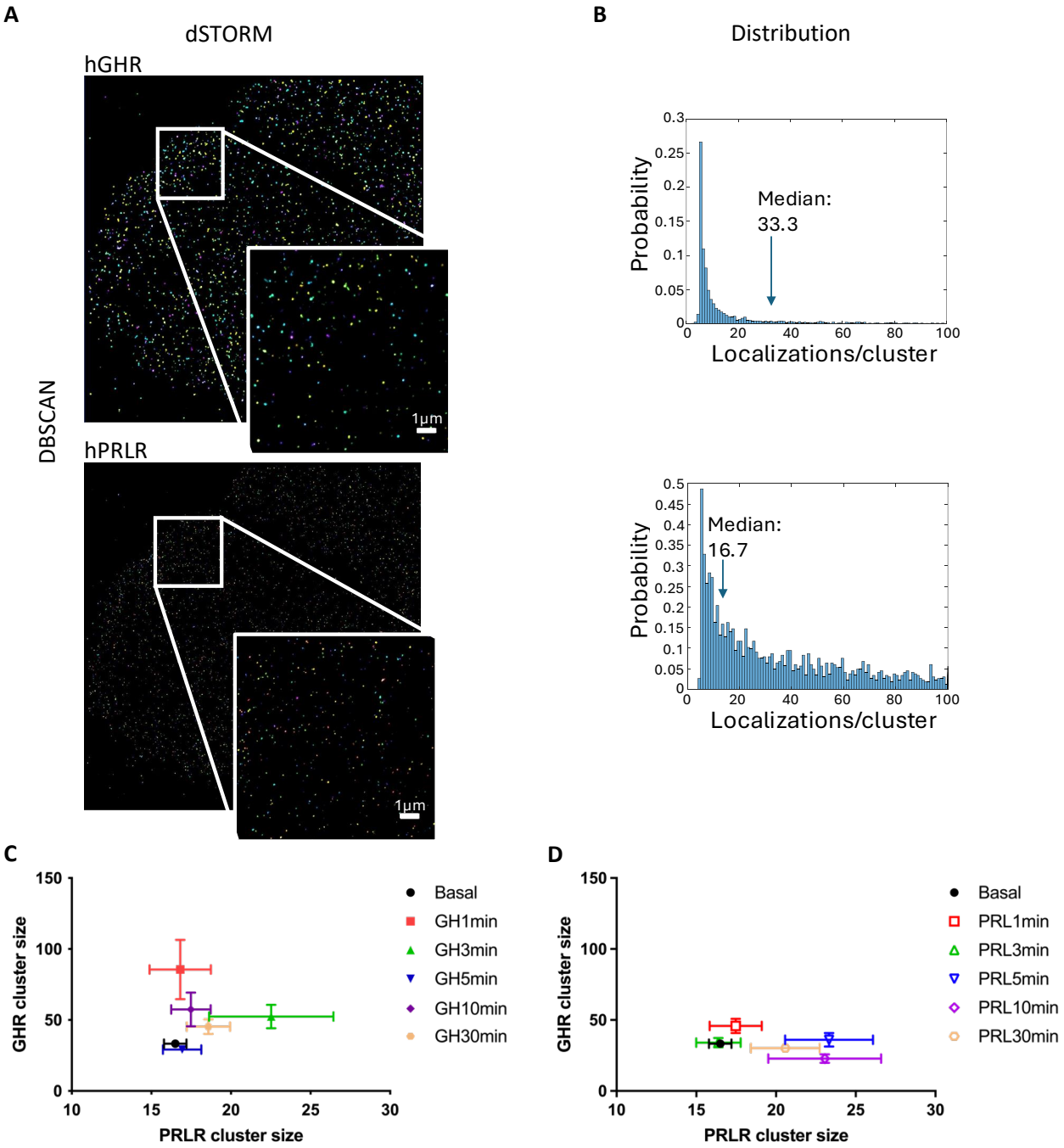

Fig. 3. GH/PRL stimulation induces a redistribution of hGHR and hPRLR clusters. **(A)** Sample dSTORM images and application of DBSCAN to identify and measure clusters (scale bar, 1 µm). To distinguish different clusters, each cluster has a different color assigned. **(B)** For similar images corresponding histograms of the relative frequencies of localizations are shown. Median cluster sizes are indicated. **(C, D)** The medians of hGHR and hPRLR cluster sizes following GH (C) and PRL (D) treatment are summarized in these plots. The x-axis and y-axis represent hPRLR and hGHR cluster sizes (counts), respectively. Data are collected from at least 6 cells from each group and displayed as median ± SE.

195 ## Spatial proximity of hGHR and hPRLR upon ligand stimulation

196 Nanoscale interactions of hGHR and hPRLR on the cell surface have yet to be well established. To evaluate
197 the extent of hGHR and hPRLR surface colocalization on T47D cells, we utilized proximity ligation assays
198 (PLAs). In PLAs, a positive signal appears only when two target proteins are in proximity (<40 nm). Notably,
199 individual treatment with GH or PRL for 5 min decreased the PLA signal observed in untreated cells by
200 34.4% and 28.1%, respectively (Fig. 4A), suggesting either ligand caused a reduction in the total number
201 of colocalized hGHR and hPRLR clusters. To further validate these observations, we calculated the ratio of
202 colocalized clusters in dSTORM images. Treatment with GH or PRL for 1 min reduced the proportion of
203 colocalized clusters by nearly 50% (Fig. 4B and 4C). To analyze their compositions, we plotted 3D
204 distributions for the colocalized clusters after ligand treatments (Fig. S1A and S1B). The probability of
205 observing co-localized clusters with numbers of hGHR and hPRLR that fall into certain bins is identified by
206 color and by the height of the bar on the z-axis. Following GH treatment for 1 min and 3 min, the number
207 of smallest clusters decreased, and the number of medium-sized clusters increased, suggesting a shift of
208 the bivariate distribution of co-localized cluster sizes toward medium-sized clusters (Fig. S1A). The
209 distribution of colocalized clusters after 5 min of GH treatment is similar to that at the basal state. In
210 contrast, after treatment with PRL for 3 min or more, the number of medium to large-sized clusters,
211 majoritarily containing either GHR or PRLR, decreased, while the number of smallest clusters increased
212 (Fig. S1B). Together, these results demonstrate that hGHR and hPRLR are spatially accessible to each other
213 and form receptor complexes on the T47D cell surface and that the nature of these complexes changes
214 differentially depending on the stimulating ligand.

215

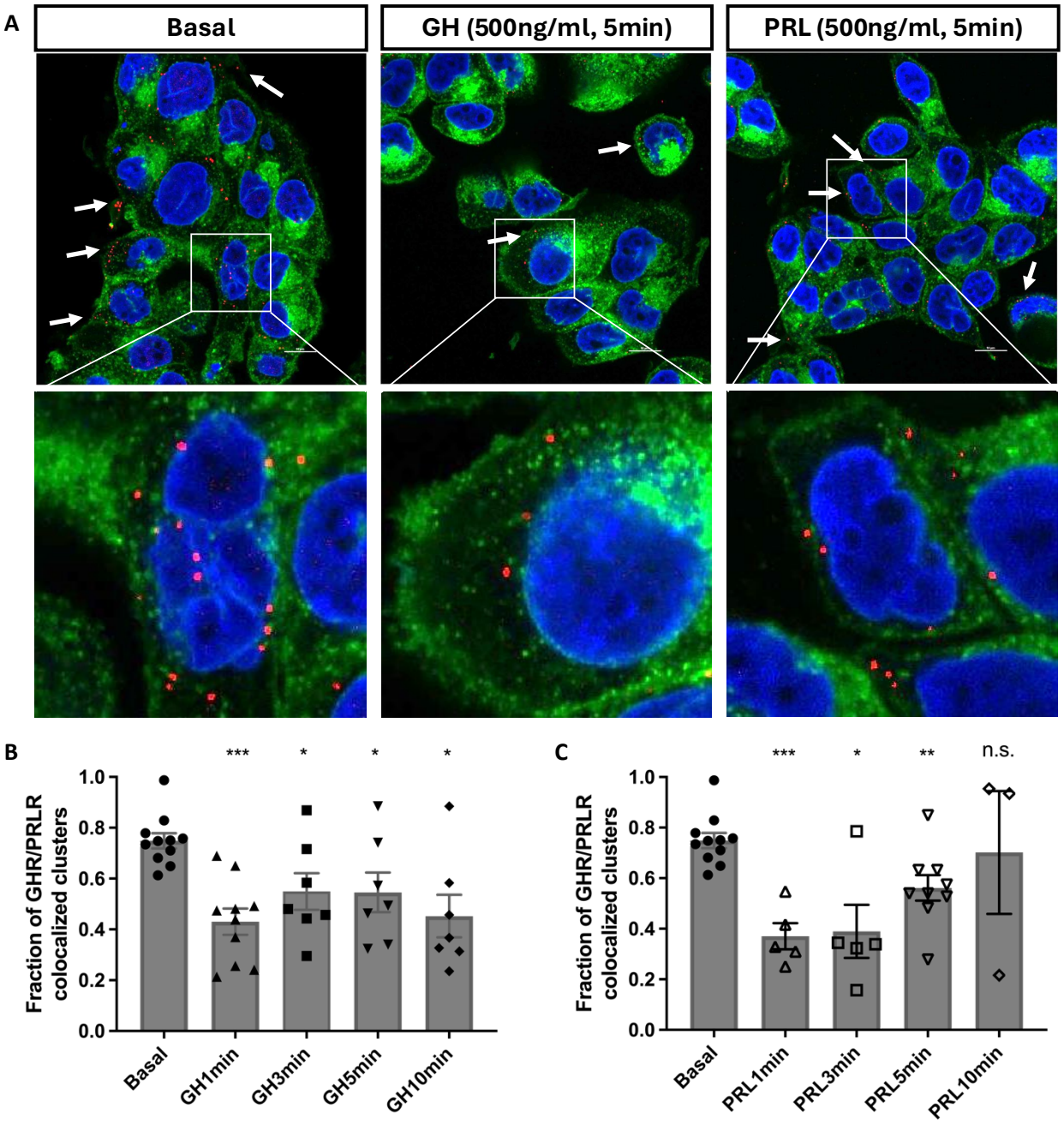

Fig. 4. Spatial proximity of hGHR and hPRLR upon ligand stimulation. **(A)** Proximity ligation assays were performed in T47D cells (scale bar, 10 µm). Here we show representative confocal microscopy images of T47D cells at resting and ligand stimulation conditions. The PLA signal (red dots) corresponds to hGHR and hPRLR complexes. Wheat germ agglutinin staining (green) was used to label glycoproteins for cell membrane imaging. DAPI (blue staining) corresponds to cell nuclei. Zoom-in views are provided in the second row. **(B, C)** hGHR and hPRLR colocalization changes in T47D cell surface following 500 ng/ml GH (B) or PRL (C) treatment obtained from dSTORM images using DBSCAN. Each data point represents a ratio of the number of clusters containing both hGHR and hPRLR, over the total number of clusters on the cell surface. Data are displayed as mean ± SE. * ($P<0.05$), ** ($P<0.01$), and *** ($P<0.001$) indicate the statistical significance in comparison with Basal and are calculated by a two-tailed t-test assuming unequal variance.

226 ## Reduction of hGHR induced by PRL on the cell surface is dependent on the presence
227 of PRLR

228 PRL strongly binds PRLR but not GHR. Yet, PRL induces a decrease of hGHR on the surface of cells
229 expressing both hGHR and hPRLR. Thus, we sought to investigate the effect of PRL on hGHR in the absence
230 of hPRLR. We utilized CRISPR/Cas9 technology to generate hPRLR knockout T47D cells (termed $T47D_{\Delta PRLR}$).
231 In addition, to evaluate isolated hPRLR responses to ligands, we also generated hGHR knockout T47D cells
232 (termed $T47D_{\Delta GHR}$). Immunoblot analysis with specific GHR and PRLR antibodies confirmed the absence of
233 hPRLR in $T47D_{\Delta PRLR}$ cells and hGHR in $T47D_{\Delta GHR}$ cells (Fig 5A). Similar to our results with parental T47D cells,
234 GH treatment of $T47D_{\Delta PRLR}$ cells rapidly reduces the density of surface hGHR, suggesting that hPRLR need
235 not be present to allow this GH-induced effect (Fig 5B). However, contrary to findings in parental T47D
236 cells, PRL treatment of $T47D_{\Delta PRLR}$ cells fails to modulate hGHR surface density (Fig 5C). Like parental T47D
237 cells, treatment of $T47D_{\Delta GHR}$ cells with GH (Fig 5D) or PRL (Fig 5E) yielded increased hPRLR surface
238 localizations. Thus, we conclude that the PRL-induced decrease of hGHR in T47D cells is dependent on the
239 presence of hPRLR, but the ability of both GH and PRL to increase surface hPRLR in T47D cells is
240 independent of hGHR's presence.

241 To extend our observations, we next examined the GH and PRL responses in a cellular reconstitution
242 system: γ2A-JAK2 [78-80] is a human JAK2-deficient fibrosarcoma cell line reconstituted with JAK2 that
243 stably expresses JAK2 but lacks hGHR and hPRLR. To independently study the role of each receptor in this
244 setting, we used our previously generated stable transfectants of γ2A-JAK2 cells that harbor either hGHR
245 or hPRLR [81] and verified the presence of the indicated receptor by immunoblotting (Fig. 5F). Consistent
246 with the observation in $T47D_{\Delta PRLR}$ cells, γ2A-JAK2-hGHR cells responded with a loss of surface hGHR density
247 to GH stimulation but not to PRL stimulation (Fig. 5G). Interestingly, as in $T47D_{\Delta GHR}$ cells, treatment of γ2A-
248 JAK2-hPRLR cells with either GH or PRL (Fig. 5H) promotes increased surface hPRLR. Thus, our findings in
249 both cell systems suggest that hPRLR-hGHR interaction, direct or indirect, is indispensable for PRL-induced
250 but not for GH-induced loss of surface hGHR.

251

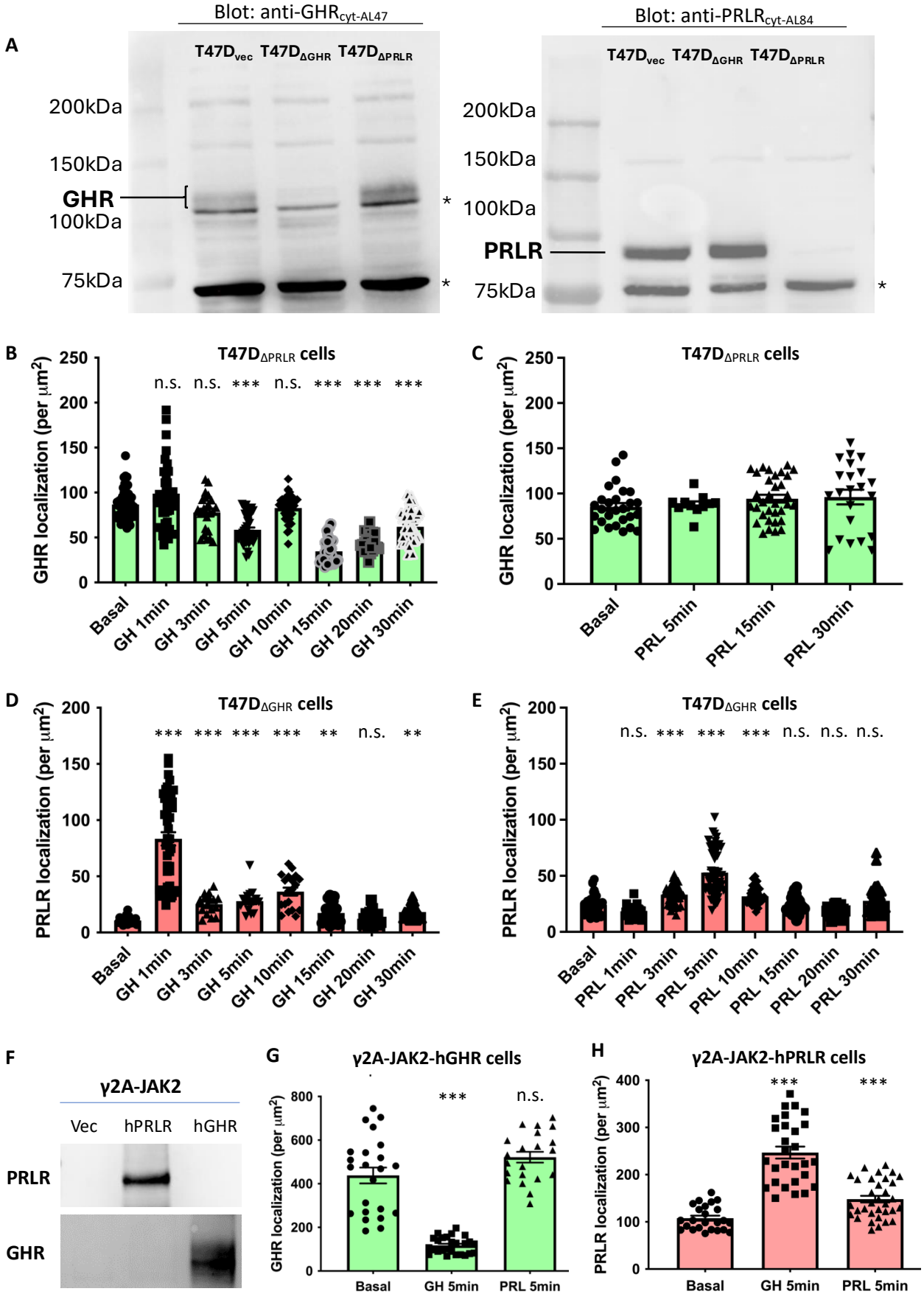
A
Blot: anti-GHRcyt-AL47
T47Dvec T47DΔGHR T47DΔPRLR
200kDa
150kDa
GHR
100kDa
75kDa
Blot: anti-PRLRcyt-AL84
T47Dvec T47DΔGHR T47DΔPRLR
200kDa
150kDa
100kDa
PRLR
75kDa
B
T47DΔPRLR cells
GHR localization (per μm2)
n.s. n.s. *** n.s. *** *** ***
Basal GH 1min GH 3min GH 5min GH 10min GH 15min GH 20min GH 30min
C
T47DΔPRLR cells
GHR localization (per μm2)
Basal PRL 5min PRL 15min PRL 30min
D
T47DΔGHR cells
PRLR localization (per μm2)
*** *** *** *** ** n.s. **
Basal GH 1min GH 3min GH 5min GH 10min GH 15min GH 20min GH 30min
E
T47DΔGHR cells
PRLR localization (per μm2)
n.s. *** *** *** n.s. n.s. n.s.
Basal PRL 1min PRL 3min PRL 5min PRL 10min PRL 15min PRL 20min PRL 30min
F
γ2A-JAK2
Vec hPRLR hGHR
PRLR
GHR
G
γ2A-JAK2-hGHR cells
GHR localization (per μm2)
*** n.s.
Basal GH 5min PRL 5min
H
γ2A-JAK2-hPRLR cells
PRLR localization (per μm2)
*** ***
Basal GH 5min PRL 5min

252

253 **Fig. 5.** PRL-induced reduction of hGHR on the cell surface depends on the presence of PRLR. **(A)** Detergent
254 cell extracts of $T47D_{vec}$, $T47D_{\Delta GHR}$, and $T47D_{\Delta PRLR}$ were analyzed by immunoblotting with anti-$GHR_{cyt\text{-}AL47}$
255 and anti-$PRLR_{cyt\text{-}AL84}$ antibodies. The bands corresponding to GHR and PRLR are annotated. Asterisks
256 indicate migration of strong non-specific bands detected in the Western Blots, which serves as a loading
257 control for protein. **(B)** In $T47D_{\Delta PRLR}$, GH (500 ng/ml) induces downregulation of hGHR localizations on the
258 cell surface, while **(C)** PRL does not change hGHR localizations. **(D, E)** In $T47D_{\Delta GHR}$ cells, GH (D) and PRL (E)
259 incite an increase of hPRLR on the cell surface. Data are displayed as mean ± SE. * (P<0.05), ** (P<0.01),
260 and *** (P<0.001) indicate the statistical significance in comparison with Basal and are calculated by a
261 two-tailed t-test assuming unequal variance. **(F)** γ2A-JAK2 cells with stable expression of hGHR or hPRLR.
262 Detergent extracts were resolved by SDS-PAGE and immunoblotted with anti-$GHR_{cyt\text{-}AL47}$ and anti-$PRLR_{cyt\text{-}}$
263 $_{AL84}$ antibodies. Vec corresponds to stable transfection with empty vector. **(G, H)** Serum-starved γ2A-JAK2-
264 hGHR cells (G) or γ2A-JAK2-hPRLR cells (H) were treated with GH (500 ng/ml) or PRL (500 ng/ml) for 5 min.
265 Localizations of hGHR in γ2A-JAK2-hGHR cells were decreased after GH treatment while remaining the
266 same after PRL treatment compared to the basal state. Localizations of hPRLR in γ2A-JAK2-hPRLR cells
267 were increased by GH or PRL treatment. Data are displayed as mean ± SE. * (P<0.05), ** (P<0.01), and ***
268 (P<0.001) denote the statistical significance in comparison with Basal and are calculated by a two-tailed
269 t-test assuming unequal variance.

270

271

Box 1 region in hPRLR contributes to PRL-induced cell surface GHR downregulation

The hPRLR-dependent PRL-induced downregulation of cell surface hGHR indicates that hPRLR can modulate the density of hGHR on the cell surface in response to PRL. To investigate this interaction, we generated a set of truncation or deletion mutants of hPRLR: (1) hPRLR-tr292, which truncates the intracellular domain of hPRLR distal to the membrane-proximal intracellular domain box 1 element; (2) hPRLR-tr238, which contains only 4 amino acids (aa) of the proximal intracellular domain and does not include box 1; and (3) hPRLR-Δbox1, in which the box 1 region (243aa-251aa) is internally deleted (shown in Fig. 6A). Expression of hPRLR-tr292, hPRLR-tr238, and hPRLR-Δbox1, as well as wild-type hPRLR, was detected by immunoblotting using monoclonal antibodies targeting the ECD of PRLR ($mAb_{ext-1.48}$). Since hPRLR-tr238 contains only 4 aa in its ICD, no immunoblot signal was detected using a polyclonal antibody (Ab_{AL-84}) targeting the hPRLR ICD. In contrast, the expression of hPRLR-tr292 was easily detected by Ab_{AL-84} (Fig. 6B). We then transiently transfected each hPRLR construct into the γ2A-JAK2-hGHR cells, which stably express hGHR, and analyzed the changes of cell surface hGHR localizations. In cells expressing wild-type hPRLR (hPRLR-WT), the localizations of hGHR significantly decreased 3 min post-exposure to GH and PRL (Fig. 6C). Similarly, under the same treatment, in cells expressing hPRLR-tr292, the localization of hGHR on the cell membrane was reduced in response to each ligand (Fig. 6D). However, in hPRLR-tr238-expressing cells, the localization of hGHR was diminished by GH stimulation but slightly increased by PRL stimulation (Fig. 6E). To further investigate the role of the box1 region for hGHR and hPRLR functional interaction, we studied hPRLR-Δbox1 expressing cells and found that upon PRL treatment, hGHR localizations did not decrease on the cell surface (Fig. 6F). As a negative control, we transfected the cells with vector (pcDNA3.1). hGHR localization decreased upon GH stimulation but remained at basal levels upon PRL stimulation (Fig. 6G). In addition, in hPRLR-ΔBox1 and hGHR expressing cells, the JAK2 and STAT5 tyrosine phosphorylation levels were assessed in response to GH and PRL stimulations. Treatment of 500ng/ml GH induces a dramatic increase in both JAK2 and STAT5 phosphorylation. In contrast, 500ng/ml PRL treatment does not cause JAK2 or STAT5 phosphorylation (Fig. 6H), consistent with PRLR Box1 being required for effective coupling of PRL occupancy of PRLR to activation of JAK2 and phosphorylation of STAT5 and the inability of PRL to signal via GHR.

Next, we analyzed colocalization in each group. In the resting state, the ratios of GHR-PRLR-colocalization clusters are relatively higher in hPRLR-WT- and hPRLR-tr292-expressing cells in comparison with hPRLR-tr238- and hPRLR-ΔBox1-expressing cells (Fig. 6I). This suggests that the box 1 region in hPRLR plays a critical role in stabilizing the hGHR-hPRLR complexes in the basal state.

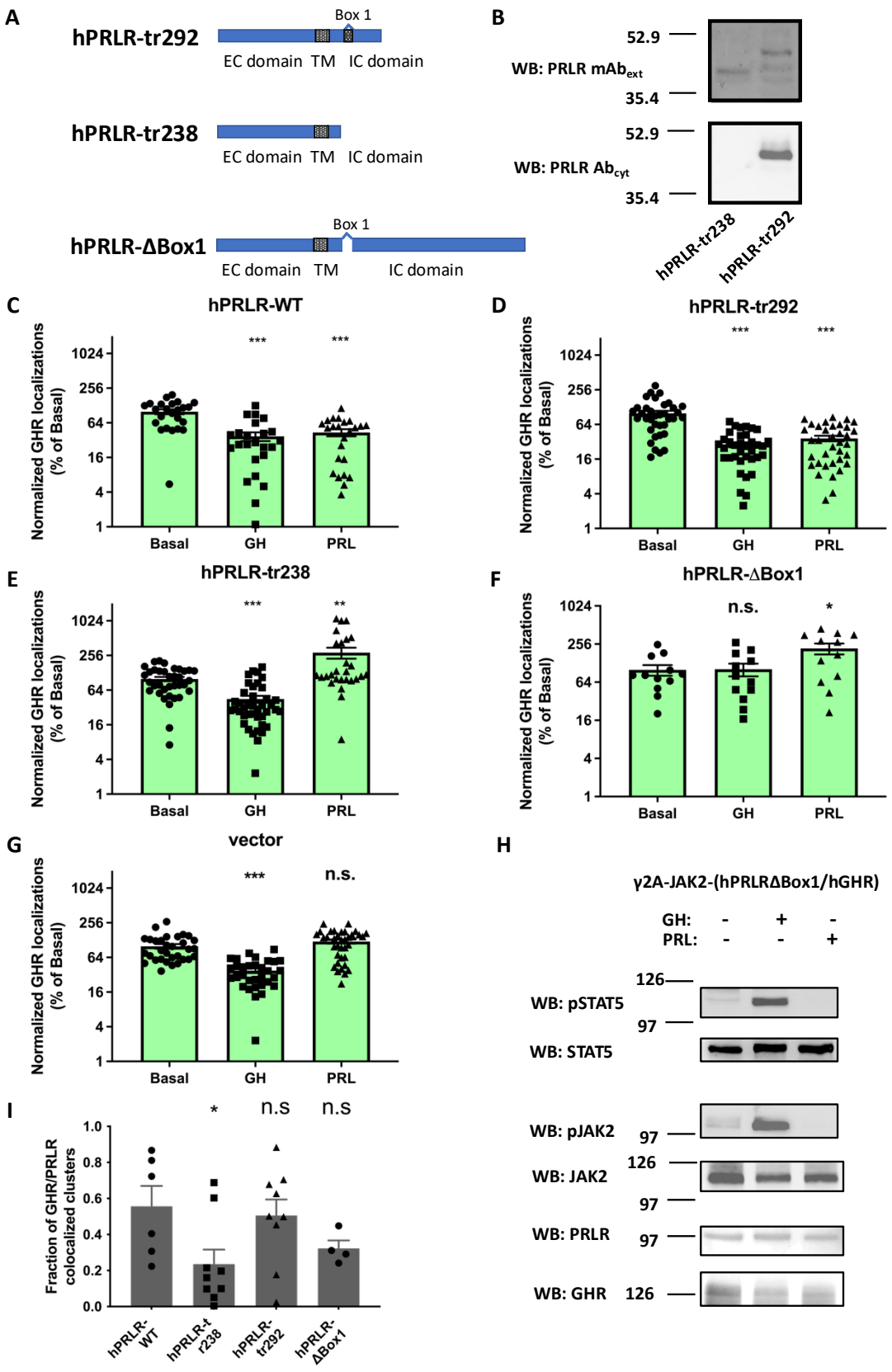
A
hPRLR-tr292
Box 1
EC domain TM IC domain
hPRLR-tr238
EC domain TM IC domain
hPRLR-ΔBox1
Box 1
EC domain TM IC domain
B
52.9
WB: PRLR mAb$_{ext}$
35.4
52.9
WB: PRLR Ab$_{cyt}$
35.4
hPRLR-tr238
hPRLR-tr292
C
hPRLR-WT
Normalized GHR localizations (% of Basal)
1024
256
64
16
4
1
***
***
Basal
GH
PRL
D
hPRLR-tr292
***
***
E
hPRLR-tr238
***
**
F
hPRLR-ΔBox1
n.s.
*
G
vector
***
n.s.
H
γ2A-JAK2-(hPRLRΔBox1/hGHR)
GH: - + -
PRL: - - +
126
WB: pSTAT5
97
WB: STAT5
WB: pJAK2
97
126
WB: JAK2
97
WB: PRLR
97
WB: GHR
126
I
Fraction of GHR/PRLR colocalized clusters
1.0
0.8
0.6
0.4
0.2
0.0
*
n.s
n.s
hPRLR-WT
hPRLR-tr238
hPRLR-tr292
hPRLR-ΔBox1

303

304 **Fig. 6.** Box 1 region in hPRLR contributes to PRLR-induced downregulation of cell surface GHR. **(A)**
305 Diagrams of employed mutant hPRLR variants with truncations or deletion in the intracellular domain.
306 ECD, extracellular domain; TMD, transmembrane domain; ICD, intracellular domain. **(B)** γ2A-JAK2-hGHR
307 cells were transiently transfected with hPRLR-tr292 and hPRLR-tr238. Cell extracts were resolved by SDS-
308 PAGE and blotted with anti-PRLR $mAb_{ext-1.48}$ and anti-$PRLR_{cyt-AL84}$. **(C-G)** γ2A-JAK2-hGHR cells were
309 transfected with (C) wild-type hPRLR (hPRLR-WT), (D) hPRLR truncated at 292 aa (hPRLR-tr292), (E) hPRLR
310 truncated at 238 aa (hPRLR-tr238), (F) hPRLR with box1 motif deleted (hPRLR-ΔBox1) and (G) vector
311 pcDNA3.1 (vector). Transfected cells were imaged by dSTORM microscopy and analyzed using the DBSCAN
312 algorithm. The density of hGHR localizations on the cell surface was calculated. Each data point represents
313 the density of hGHR in a cell surface area of size 6.25 µm X 6.25 µm. Data are collected from at least 6
314 cells (4 ROIs per cell) from each group, and values are displayed as mean ± SE (from three independent
315 experiments). Data are normalized such that the basal is 100%. * ($P<0.05$), ** ($P<0.01$), and *** ($P<0.001$)
316 denote the statistical significance in comparison with Basal and are calculated by a two-tailed t-test
317 assuming unequal variance. **(H)** Detergent cell extracts of hPRLR-ΔBox1 and hGHR-expressing cells were
318 analyzed by immunoblotting. After 5 hrs. starvation, cells were treated with GH (500 ng/ml) or PRL (500
319 ng/ml) for 10 min. In each experiment, the average Basal value is considered 100%. **(I)** Fraction of
320 GHR/PRLR colocalized clusters. In the resting state, the colocalization ratio is significantly lower for cells
321 expressing hPRLR-tr238 than for those expressing hPRLR-WT. Each data point represents the ratio of the
322 number of clusters, which contain both hGHR and hPRLR, to the total number of clusters on the cell
323 surface. Data are displayed as mean ± SE. * ($P<0.05$) indicates statistical significance in comparison with
324 WT and is calculated by a two-tailed t-test assuming unequal variance (all bars without an asterisk are not
325 significant).

326

327 Box 1 region in hGHR plays an essential role in regulating PRLR and GHR interaction

328 From our observations (Fig. 6), we concluded that the JAK2 binding site, i.e., the box 1 region, in hPRLR is
329 required for PRL-induced hGHR down-regulation from the cell surface. To further assess whether the JAK2
330 binding site on hGHR is also essential, we generated hGHR-ΔBox1, in which the box 1 region (297aa –
331 305aa) was deleted (Fig. 7A). In cells expressing both hGHR-ΔBox1 and hPRLR we observed that GH does
332 not alter the hGHR-ΔBox1 localizations on the cell surface, while PRL slightly increases hGHR-ΔBox1
333 localizations (Fig. 7B). Together, these results re-affirm that binding of JAK2 to hGHR is also required for
334 hPRLR-mediated regulation of hGHR availability on the cell surface.

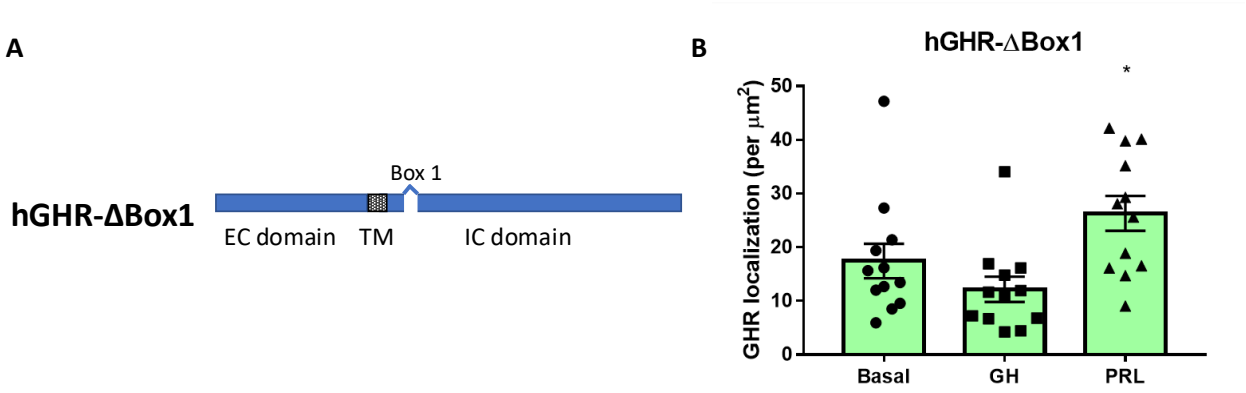

Fig. 7. Box 1 region in hGHR also plays an important role in PRLR and GHR interaction. **(A)** Diagram of hGHR-ΔBox1 showing the deleted box 1 region in the intracellular domain of hGHR. **(B)** γ2A-JAK2-hPRLR cells were transfected with hGHR-ΔBox1. Transfected cells were imaged by dSTORM microscopy and analyzed using DBSCAN. The density of hGHR localizations on the cell surface was calculated. Each data point represents the density of hGHR in a cell surface area of size 6.25 µm X 6.25 µm. Data are collected from at least 6 cells for each group and displayed as mean ± SE. * (P<0.05), ** (P<0.01), and ***(P<0.001) indicate the statistical significance in comparison with Basal and are calculated by a two-tailed t-test assuming unequal variance.

Materials and Methods:

Materials:

Common reagents were purchased from Sigma Aldrich Corp. (St. Louis, MO) unless otherwise noted. Fetal bovine serum was purchased from Atlanta Biologicals (Lawrenceville, GA). Cell culture medium, penicillin/streptomycin and trypsin were purchased from Corning (Corning, NY). Recombinant hGH was kindly provided by Eli Lilly & Co. (Indianapolis, IN). Recombinant human PRL was obtained from the National Hormone and Pituitary Program.

Antibodies:

Polyclonal anti-$GHR_{cyt\text{-}AL47}$ (1:1000) against the intracellular domain of GHR and polyclonal anti-$PRLR_{cyt\text{-}AL84}$ against the human PRLR intracellular domain described previously in [82] and [83], respectively, were used as the primary antibodies for western blot analysis. Monoclonal anti-$GHR_{ext\text{-}mAb}$ 74.3 (1:1000) against the extracellular S2 domain of GHR [40, 68, 70, 79, 81, 84-93] and monoclonal anti-$PRLR_{ext\text{-}mAb}$ 1.48 against the extracellular S2 domain of human PRLR [70] were used for microscopy. Specifically, we let hybridoma cells secrete these antibodies into the cell medium to avoid the purification step. A detailed description of the antibodies and their previous use is provided in the references. Specificity of anti-$GHR_{ext\text{-}mAb}$ and anti-$PRLR_{ext\text{-}mAb}$ 1.48 was confirmed using confocal microscopy (see also Supp. Fig. S2-S4). The following secondary antibodies were used: Alexa Fluor 568 goat anti-mouse IgG1 (Invitrogen #A-21124) (1:1000), Alexa Fluor 647 goat anti-mouse IgG2b (Invitrogen #A-21242) (1:1000), Alexa Fluor 647 goat anti-mouse IgG1 (Invitrogen #A-21240) (1:1000) and Alexa Fluor 568 goat anti-mouse IgG2b (Invitrogen # A-21144)

363 (1:1000). In the absence of primary antibodies, secondary antibodies did not show any fluorescence
364 signals (see also Supp. Fig. S3).

365 Cloning and constructs:

366 The human GHR cDNA in pcDNA1 was a generous gift from R. Ross (University of Sheffield, Sheffield, UK).
367 The human PRLR cDNA in pEF/V5/HIS was generously provided by C. Clevenger (Virginia Commonwealth
368 University, Richmond, VA). hPRLR-tr238 and hPRLR-tr292 were generated by amplifying with external
369 primers containing EcoRI site and a stop codon with XhoI site after the sequence of 238 or 292 amino acid,
370 respectively. hPRLR-ΔBox1, and hGHR-Δbox1 were generated by overlap extension polymerase chain
371 reaction (PCR) with associated primers and cloned into pcDNA3.1(+) vector.

372 Cell culture and transfections:

373 Human T47D breast cancer cells were purchased from American Type Culture Collection (Manassas, VA).
374 Cells were maintained in RPMI 1640 medium supplemented with 10% fetal bovine serum (FBS), 100
375 units/ml penicillin and 100 µg/ml streptomycin in a humidified atmosphere of 5% CO2 and 95% air at 37 °C.

376 γ2A-JAK2 cells were generated by transfection of γ2A cells [78] with pcDNA3.1(+)/zeo-JAK2 and
377 maintained in culture, as described previously [79, 80]. The generation of γ2A-JAK2-GHR and γ2A-JAK2-
378 PRLR cells has been previously described [81].Transient expression of receptors was achieved by using
379 Lipofectamine LTX Plus (Invitrogen), transfecting 0.3 pmol plasmid DNA per 6-cm^2 dish.

380 Western blot

381 Cells were serum starved for 5 hours and treated with 500 ng/ml GH or 500 ng/ml PRL at 37 °C for 10 min.
382 Stimulations were terminated by washing the cells with ice-cold phosphate-buffered saline supplemented
383 with 0.4 mM sodium orthovanadate. Cells were lysed in lysis buffer for 30 min at 4°C. Then cell lysates
384 were centrifuged at 15,000 g for 10 min at 4°C. The protein extracts (supernatant) along with SDS sample
385 buffer were resolved by SDS-PAGE.

386 Sample preparation for imaging:

387 Cells were seeded into either eight well #1.5 coverslip bottom dishes (Ibidi) or 25 mm #1.5 coverslips
388 (Electron Microscopy Sciences). Cells were serum starved for 5 hours, then treated with GH (500 ng/ml),
389 PRL (500 ng/ml) at 37 °C for the indicated time. Then the cells were washed with Dulbecco's Phosphate-
390 Buffered Saline (DPBS) three times and fixed with 4% PFA (paraformaldehyde) in 1X DPBS with calcium
391 and magnesium (Cat # 21-030-CV) for 10 min. After multiple washes with DPBS, cells were blocked with
392 5% normal horse serum, 5% normal goat serum, 5% BSA for 30 min. Lastly, cells were incubated in primary
393 antibody for 3h and secondary antibody for 70 min at 37°C.

394 dSTORM imaging and data analysis

395 dSTORM experiments were conducted on an inverted Nikon Ti2 N-STORM microscope equipped with a
396 100 X 1.49 NA oil immersion objective (Nikon, Japan), 488 and 647 nm lasers, and an iXon DU-897 Ultra
397 EMCCD camera (Andor, Oxford Instruments). The dSTORM imaging buffer consists of two buffers, A and
398 B, and a GLOX mixture. Buffer A is made of 10 mM Tris pH 8 and 50 mM NaCl, while buffer B is made of

399 50 mM Tris pH 8 and 10 mM NaCl. The GLOX mixture consists of 14 mg glucose oxidase (Sigma, St Louis,
400 Missouri), 50 µl catalase (17 mg/ml) (Roche, Penzberg, Germany), and 200 µl of Buffer A. The dSTORM
401 buffer is made by combining (on ice) 7 µl GLOX with 7 µl 2-mercaptoethanol (Sigma, St Louis, Missouri)
402 and 690 µl Buffer B, using only the supernatant from the GLOX mixture. For a detailed description of the
403 buffer, we refer the reader to [94].

404 The cell membrane was focused using TIRF excitation, which selectively images within 100-150 nm of the
405 cell membrane, making it an excellent method to study surface distribution of membrane proteins. Of
406 note, TIRFM exploits the unique properties of an induced evanescent field in a limited specimen region
407 immediately adjacent to the interface between two media having different refractive indices. It thereby
408 dramatically reduces background by rejecting fluorescence from out-of-focus areas in the detection path
409 and illuminating only the area right near the surface.

410 Moreover, we reduced auto-fluorescence by ensuring that (a) cells are grown in phenol-red-free media,
411 (b) imaging is performed in STORM buffer which reduces autofluorescence, and (c) our immunostaining
412 protocol includes a quenching step aside from using blocking buffer with different serum, in addition to
413 BSA (5%). Moreover, we employed extensive washing steps following antibody incubations to eliminate
414 non-specifically bound antibodies. Ensuring that the TIRF illumination field is uniform helps reduce scatter.
415 Additionally, an extended bleach step prior to the acquisition of frames to determine localizations helped
416 further reduce the probability of non-bleached fluorescent molecules.

417 For dual color STORM imaging, the sample was illuminated with alternating 561 nm or 647 nm lasers and
418 40,000 frames of images were acquired per channel (9ms/frame). The chromatic offset associated with
419 the different acquisition wavelengths was corrected using 0.1 µm microspheres [95, 96]. Imaging captured
420 the fluorophores' blinking events. Localizations were counted as true localizations, when at least 5
421 consecutive blinking events had been observed. Moreover, coordinates were filtered using a threshold
422 radius of 25nm. dSTORM images were reconstructed using the built-in STORM module in NIS-Elements
423 (Nikon). Nikon software was used for Gaussian fitting, and each dot represents the peak of a Gaussian.
424 The localizations list was exported and further analyzed in *Matlab*. In particular, for the DBSCAN cluster
425 analysis, we employed Clus-DoC directly on the list of localizations, utilizing the parameters of a minimum
426 of 4 neighbors within a cluster radius of 20nm [97].

427 Proximity Ligation Assay

428 Cells were serum starved for 5 hours, then treated with GH (500 ng/ml) or PRL (500 ng/ml) at 37 °C for
429 the indicated time. Then the cells were washed with DPBS three times and fixed with 4% PFA
430 (paraformaldehyde) for 10 min. After multiple washes with DPBS, cells were blocked with 5% normal
431 horse serum, 5% normal goat serum, 1% BSA for 30 min. Lastly, cells were incubated in primary antibody
432 for 3h and secondary antibody for 70 min at 37°C. After secondary antibody incubation, ligation and
433 amplification were performed according to the manufacturer's protocol (Duolink® PLA; Sigma-Aldrich).
434 Briefly, ligation solution containing ligase was added to the samples, followed by incubation for 30
435 minutes at 37°C. Samples were then washed and incubated with the amplification solution, which includes
436 polymerase, at 37°C for 100 minutes to amplify the PLA signal.

437

Generating hGHR knockout and hPRLR knockout T47D cells

We utilized CRISPR/Cas9 to generate $T47D_{\Delta PRLR}$ and $T47D_{\Delta GHR}$. Two single-guide RNAs (sgRNAs) and Cas9 nickase (Cas9n) were designed to create sticky-end double-strand breaks in DNA at the targeted locus, triggering DNA repair via the Non-Homologous End Joining (NHEL) pathway, which introduces insertions, deletions or frameshift mutations [98]. Each sgRNA was expressed using plasmid #62987 pSpCas9n(BB)-2A-Puro(PX462) V2.0 (purchased from Addgene), which also expressed Cas9n when transfected into cells. Two vectors, built on pSpCas9n(BB)-2A-Puro(PX462) V2.0 backbone, containing a pair of sgRNAs targeting either the hGHR or hPRLR gene for knockout, as well as a built-in Cas9n gene, were transfected into newly purchased T47D cells. The transfected cells were plated at serial dilutions and selected with puromycin. Single clones were picked and expanded. The vector backbone pSpCas9n(BB)-2A-Puro(PX462) V2.0 was also used for transfection into T47D cells as a control cell line.

Genomic DNA was extracted from each clone. Primers were designed 200-400 bp upstream and downstream of the targeted locus of the hGHR or hPRLR gene to amplify the genomic DNA via PCR, which was subsequently cloned into the pUC19 vector for sequencing. Clones with mutations on both alleles were identified, and the western blot was used to confirm the absence of expression of the targeted genes.

Design of sgRNAs for hGHR or hPRLR knockout

A pair of 20 bp sequences located 10-25 bp apart at the target locus was chosen using the Feng Zhang lab's Target Finder [99]. This tool identified the best pair of guide RNA sequences with theoretically zero off-target effects. One sequence targeted the top strand, and the other targeted the bottom strand, enabling the introduction of a sticky-end double-strand DNA break. Each guide RNA sequence was synthesized as double-stranded oligonucleotides with a CACC at 5’ overhand of the 20-nt guide sequence and an AAAC at the 5’ overhand of the complementary strand, allowing insertion into the backbone plasmid pSpCas9n(BB)-2A-Puro(PX462) V2.0 using the BbsI restriction enzyme. An extra nucleotide ‘G’ was added to the 5’ end of the 20-nt guide if the sequence did not begin with ‘G’, which is the preferred first base following the U6 RNA Polymerase III promoter.

The target locus for introducing mutations in the hGHR gene was located at exon 4. Exon 4 was chosen because many naturally occurring pathological mutations in Laron Syndrome are located in this region. Additionally, deletion of the 3’ end of exon 4 and its adjacent intron has been shown to successfully generate GHR knockout mice[100]. The hPRLR gene has seven isoforms; exon 5 is included in six of these isoforms, except for the ΔS1 PRLR isoform, in which both exons 4 and 5 are skipped by alternative splicing. Therefore, we selected the end of exon 5 and the adjacent intron as the target locus for introducing mutations. The goal was to knock out all six isoforms containing exon 5, as well as the ΔS1 PRLR isoform, by interrupting alternative splicing. This was achieved by deleting the initial GU dinucleotide sequence at the 5’ end of the intron, which is required for the binding of the U1 protein of the spliceosome.

Statistical analysis

Imaging and biochemical experiments were carried out at least three times to ensure reproducibility. Data were analyzed using unpaired, two-tailed t-tests. *Prism* software was used for statistical analysis (GraphPad Inc, USA). Data are presented as means ± s.e.m.

476 To quantify changes in localization and colocalization we randomly selected 4 ROIs (regions of interest)
477 per cell to calculate fractions and then calculated the average of three different cells from independently
478 repeated experiments.

479

480 Discussion:

481 The non-ligand-bound states of hGHR and hPRLR have been extensively investigated. Pre-
482 homodimerization of hGHR and hPRLR has been reported using structural and biochemical methods [40,
483 101-104]. At the same time, a recent study supports the notion that GHR, at physiological densities, exists
484 as monomers on the cell surface and becomes activated by a ligand-induced dimerization [105]. The
485 current study uses a highly precise and sensitive single-molecule localization microscopy approach to
486 study the formation of hGHR and hPRLR nanoclusters and the cell surface receptor availability. Our super-
487 resolution images reveal that in human T47D breast cancer cells and the γ2A-JAK2 cell exogenous
488 expression system, the cluster size of hGHR and hPRLR in the basal state range from a few localizations
489 per cluster up to a thousand localizations per cluster.

490 With GH or PRL treatment, the number of hGHR on both T47D and γ2A-JAK2 cell surfaces is decreased,
491 indicating the removal of surface hGHR. Moreover, the distribution curve of hGHR shifts toward larger
492 cluster sizes (Fig. 3), suggesting a ligand-induced aggregation of receptors. In turn, hPRLR numbers
493 dramatically increase on the cell surface in response to ligand stimulation. The newly presented hPRLR
494 clusters may impact the distribution of cluster sizes, which may explain why the median of hPRLR cluster
495 sizes does not change much with ligand treatment.

496 Our PL assay data indicate that distances between hGHR and hPRLR are small (less than 40nm). This
497 implies that hGHR and hPRLR form co-localized clusters in unstimulated states, suggesting hGHR and
498 hPRLR are physically accessible to one other. With GH stimulation, the fraction of co-localized receptors
499 is decreased. Given that GH treatment enhances the coimmunoprecipitation of total cellular hGHR and
500 hPRLR [68], the decrease in co-localized surface receptors can likely be attributed to removing co-localized
501 receptors from the cell surface.

502 It is well documented that hPRLR is engaged by both PRL and GH, while hGHR only responds to GH [41,
503 43, 44]. Unexpectedly, we found that PRL induces a down-regulation of cell surface hGHR in cells that co-
504 express hGHR and hPRLR (Fig. 2), indicating that hPRLR directly or indirectly interacts with hGHR.
505 Interestingly, PRL was unable to induce hGHR down-regulation in cells either lacking hPRLR or expressing
506 hPRLR without its Box1 region (hPRLR-tr238 or hPRLR-ΔBox1), suggesting that JAK2 and PRLR association
507 is required for hGHR-hPRLR interaction that in turn allows PRL-induced downregulation of cell surface
508 hGHR. Notably, previous work showed that GHR and JAK2 association is necessary for JAK2 to stabilize
509 cell surface GHR and inhibit constitutive GHR down-regulation [80]. Furthermore, single-particle tracking
510 studies showed that, in the presence of JAK2, a higher level of ligand-induced dimerization of GHR was
511 observed [105]. Moreover, JAK2 with intact kinase activity is required for GH-induced GHR down-
512 regulation [80]. Similarly, the box1 region of PRLR also associates with JAK2, and deletion or modulation
513 of the last proline residue of box1 abrogates PRLR function [106]. Collectively, these findings suggest that
514 the box1 regions in hGHR and hPRLR play a crucial role in the transduction of the individual signaling
515 cascades and hGHR-hPRLR association.

516 Here we found that, in the resting state, the degree of hGHR-hPRLR colocalization is higher in cells
517 expressing hPRLR with the box1 motif. This suggests JAK2 may not only stabilize GHR but also support the
518 formation of hGHR-hPRLR-containing clusters. Previously, it has been suggested that such clusters are
519 comprised of hGHR homodimers and hPRLR homodimers that together form (hGHR-hGHR) – (hPRLR-
520 hPRLR) hetero-multimers or higher order oligomers [69]. Indeed, because the intracellular domains (ICD)
521 of both hGHR and hPRLR are highly disordered, the flexibility of their ICDs may provide room for recruiting
522 JAK2 and stabilizing the hGHR-hPRLR association [107, 108]. Moreover, a study of the crystal structure of
523 erythropoietin receptor (EPOR) and leptin receptor (LEPR), which also belong to the class I cytokine
524 receptor family, revealed recently that JAK2/EPOR and JAK2/LEPR complexes contained four JAK2 and
525 four EPOR or LEPR molecules, respectively [109]. Hence, it is possible that hGHR-hGHR homodimers and
526 hPRLR-hPRLR homodimers form complexes in a similar fashion (Fig. 8). We propose that this JAK2/Box1-
527 mediated interaction of receptors is not limited to hGHR and hPRLR but may generalize to other receptors
528 of the class I cytokine receptor family. We note, however, that determinants within particular receptors
529 (perhaps residing in their extracellular and/or transmembrane domains) and their intracellular JAK2
530 association domains may facilitate, to varying degrees, their propensity to form multimeric aggregates.
531 GHR and PRLR, for example, may tend to do so more avidly with each other than either one does with
532 other cytokine receptors. Additional studies are required to determine and understand the modes and
533 functions of the hGHR-hPRLR association.

534 An obvious question is to what extent our observed regulation is biologically relevant. While our work
535 does not provide an answer to this question, one could argue that, generally speaking, such a mechanism
536 could provide a means for crosstalk and feedback between the two cytokine receptors and allow for a
537 more fine-tuned signaling response. In particular high levels of PRL could reduce GH signaling thereby
538 prioritizing PRL's function over GHR-mediated growth processes. PRLR's ability to modulate GHR cell
539 surface availability might also contribute to tissue-specific responses to hormonal signals. For instance, in
540 situations with high PRL levels in circulation such as during lactation [110], downregulation of mammary
541 gland cell surface GHRs could prevent GH from counteracting PRL's effects. Also, PRL and GH have
542 important roles in metabolism, often with opposing effects [2, 111-113]. PRL promotes lipogenesis and
543 energy storage, while GH promotes lipolysis and energy mobilization. By downregulating GHRs, PRL could
544 shift the metabolic balance in favor of energy storage. Moreover, this regulation may also have disease
545 implications: hPRL/hPRLR-mediated downregulation of cell surface hGHR could be a relevant factor in the
546 observed anti-tumor effect of PRLR signaling, especially in triple-negative breast cancer (TNBC) expressing
547 PRLR but lacking other interfering hormone receptors. As previously shown, the TNBC cell lines MDA-MB-
548 231 and MDA-MB-453 show significantly increased GHR [15] while expressing no or only endogenous
549 levels of PRLR, respectively [28]. PRL treatment significantly decreased cell viability and invasive capacity
550 of MDA-MB-231 cells following the restoration of PRLR expression. In MDA-MB-453 cells, PRL caused a
551 significant reduction in cell viability. A xenograft model with inoculated MDA-MB-453 cells confirmed the
552 growth inhibitory effect of PRL treatment *in vivo*, suggesting PRLR expression as an indicator of a favorable
553 prognosis. However, several studies have reported the contrary, namely that PRL promotes breast cancer
554 [12], presenting a conundrum that so far has not been resolved. Among the observations supporting a
555 role of PRL in promoting breast cancer are: (1) frequent PRLR overexpression in BC tissues, (2) association
556 of elevated (serum) PRL with increased BC risk – in particular for estrogen receptor (ER) positive BC – and
557 increased risk for metastatic progression from epidemiologic data, and (3) PRL stimulation modulating the
558 cytoskeleton and inducing motility of human breast cancer cells (including T47D) in vitro, which has been
559 associated with mammary carcinoma progression in vivo [12]. Of note, our hypothesis of PRL-mediated

560 down-regulation of GHR presence on the cell surface being protective does not mean that other effects
561 cannot also be involved or cancel this positive effect out. Moreover, timing could be a decisive element:
562 while PRL might have a protective effect (depending on other factors) at the time of tumorigenesis, it may
563 actually facilitate BC metastasis. But given the lack of experimental data indicating a clear protective effect
564 through Jak2-mediated receptor interactions in PRLR+ GHR+ BC at any BC stage, our hypothesis remains
565 speculative.

566 Besides, observations in MCF-7, a human breast cancer cell line, where binding of PRL causes
567 internalization and downregulation of PRLR expression seem to contradict our observations in T47D cells
568 [114]. Recently, a competition between two kinases (JAK2 and LYN) for binding hGHR at the box1-box2
569 region was reported [115], indicating that hGHR nanocluster formation at the cell membrane is regulated
570 also by kinases. It is conceivable that similar kinase-dependent competition mechanisms could regulate
571 also PRLR cell surface availability. Thus, differences in cells' expression of such kinases could then play a
572 role in the perceived inconsistency. Moreover, [114] focuses on the downregulation of the long PRLR
573 isoform in response to PRL, while all other isoforms were undetectable in MCF-7 cells. So, this and other
574 differences between the cell lines may be the reason for the perceived contradiction.

575 We note that a limitation of our study is the focus on T47D and γ2A-JAK2 cells. It remains to be seen, if
576 we can observe and replicate the same effect also in other cell lines, for instance mammary epithelial cells
577 or other hGHR+ PRLR+ cancer cell lines. Also, the roles of the different membrane PRLR isoforms have not
578 been fully addressed and our study lacks isoform specific data [37]. The anti-PRLR antibody that we used
579 does not only recognize the long form PRLR but also the intermediate form and the short forms, all of
580 which have ECDs. All these forms contain the box1 motif. Importantly, form S1b is almost identical to
581 hPRLR-tr292, but behaves similarly to LF (i.e. our hPRLR WT) in terms of normalized GHR cell surface
582 localization and PRLR co-localization (Fig. 6). So, while we do not have experimental confirmation, we
583 would expect that these other isoforms behave somewhat similarly to LF with respect to GHR surface
584 membrane interactions – while still inducing different downstream effects as well as playing different
585 roles in breast cancer [37, 116-118].

586 As part of future research, we plan to study the observed effect in cell lines other than T47D. We would
587 also like to investigate if the mechanism is PRLR-GHR specific, or if there are other cytokine receptors that
588 can interact in a similar asymmetric, ligand-dependent manner, such that one regulates the other
589 receptor's surface availability. Importantly, we would like to elucidate any biological relevance of the
590 observed effect, analyze roles and consequences of PRLR isoforms, and investigate our hypothesis that
591 PRLR-mediated downregulation of cell surface GHR contributed to the anti-tumoral effect of PRL
592 treatment in PRLR-positive TNBC.

593

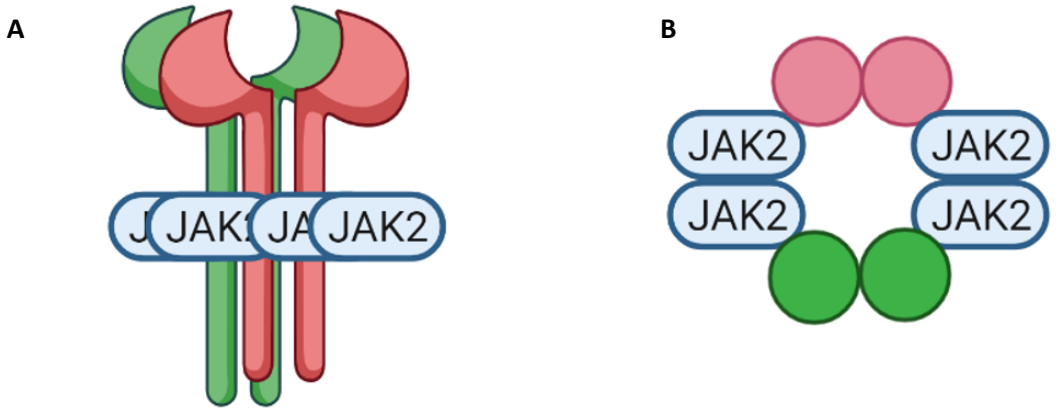

Fig. 8. Model of JAK2 stabilizing GHR-GHR and PRLR-PRLR heteromers. **(A)** Schematic representation of GHRs homodimer and PRLRs homodimer form a heteromer, which contains two PRLRs (red), two GHRs(green), and four JAK2(blue). **(B)** A top view of the JAK2/PRLR/GHR multimer.

599 Reference:

600 1. Isaksson, O.G., S. Eden, and J.O. Jansson, *Mode of action of pituitary growth hormone on target*
601 *cells.* Annu Rev Physiol, 1985. **47**: p. 483-99.
602 2. Moller, N. and J.O. Jorgensen, *Effects of growth hormone on glucose, lipid, and protein*
603 *metabolism in human subjects.* Endocr Rev, 2009. **30**(2): p. 152-77.
604 3. Brooks, C.L., *Molecular mechanisms of prolactin and its receptor.* Endocr Rev, 2012. **33**(4): p.
605 504-25.
606 4. Gonzalez-Lucano, L.R., et al., *Increased expression of the prolactin receptor is associated with*
607 *malignant laryngeal tumors.* Exp Ther Med, 2012. **3**(4): p. 603-607.
608 5. Ascencio-Cedillo, R., et al., *Prolactin and prolactin receptor expression in cervical intraepithelial*
609 *neoplasia and cancer.* Pathol Oncol Res, 2015. **21**(2): p. 241-6.
610 6. Harris, J., et al., *Prolactin and the prolactin receptor: new targets of an old hormone.* Ann Med,
611 2004. **36**(6): p. 414-25.
612 7. Asad, A.S., et al., *The role of the prolactin receptor pathway in the pathogenesis of glioblastoma:*
613 *what do we know so far?* Expert Opin Ther Targets, 2020. **24**(11): p. 1121-1133.
614 8. Sethi, B.K., G.V. Chanukya, and V.S. Nagesh, *Prolactin and cancer: Has the orphan finally found a*
615 *home?* Indian J Endocrinol Metab, 2012. **16**(Suppl 2): p. S195-8.
616 9. Boguszewski, C.L. and M. Boguszewski, *Growth Hormone's Links to Cancer.* Endocr Rev, 2019.
617 **40**(2): p. 558-574.
618 10. Strous, G.J., et al., *Growth Hormone Receptor Regulation in Cancer and Chronic Diseases.* Front
619 Endocrinol (Lausanne), 2020. **11**: p. 597573.
620 11. Chhabra, Y., M.J. Waters, and A.J. Brooks, *Role of the growth hormone-IGF-1 axis in cancer.*
621 Expert Rev Endocrinol Metab, 2011. **6**(1): p. 71-84.
622 12. Clevenger, C.V. and H. Rui, *Breast Cancer and Prolactin - New Mechanisms and Models.*
623 Endocrinology, 2022. **163**(10).
624 13. Shemanko, C.S., *Prolactin receptor in breast cancer: marker for metastatic risk.* J Mol Endocrinol,
625 2016. **57**(4): p. R153-R165.
626 14. Goffin, V., *Prolactin receptor targeting in breast and prostate cancers: New insights into an old*
627 *challenge.* Pharmacol Ther, 2017. **179**: p. 111-126.
628 15. Zhu, X., et al., *Growth hormone receptor promotes breast cancer progression via the*
629 *BRAF/MEK/ERK signaling pathway.* FEBS Open Bio, 2020. **10**(6): p. 1013-1020.
630 16. Subramani, R., et al., *Role of Growth Hormone in Breast Cancer.* Endocrinology, 2017. **158**(6): p.
631 1543-1555.
632 17. Xu, J., et al., *The role of prolactin receptor in GH signaling in breast cancer cells.* Mol Endocrinol,
633 2013. **27**(2): p. 266-79.
634 18. Gebre-Medhin, M., et al., *Growth hormone receptor is expressed in human breast cancer.* Am J
635 Pathol, 2001. **158**(4): p. 1217-22.
636 19. Mertani, H.C., et al., *Cellular expression of growth hormone and prolactin receptors in human*
637 *breast disorders.* Int J Cancer, 1998. **79**(2): p. 202-11.
638 20. Kavarthapu, R., R. Anbazhagan, and M.L. Dufau, *Crosstalk between PRLR and EGFR/HER2*
639 *Signaling Pathways in Breast Cancer.* Cancers (Basel), 2021. **13**(18).
640 21. Wang, L., et al., *Functional regulations between genetic alteration-driven genes and drug target*
641 *genes acting as prognostic biomarkers in breast cancer.* Sci Rep, 2022. **12**(1): p. 10641.
642 22. Liang, J., et al., *PRLR and CACNA2D1 Impact the Prognosis of Breast Cancer by Regulating Tumor*
643 *Immunity.* J Pers Med, 2022. **12**(12).

644 23. Fiorillo, A.A., et al., *The prolactin receptor transactivation domain is associated with steroid*
645 *hormone receptor expression and malignant progression of breast cancer.* Am J Pathol, 2013.
646 **182**(1): p. 217-33.
647 24. Schuler, L.A. and K.A. O'Leary, *Prolactin: The Third Hormone in Breast Cancer.* Front Endocrinol
648 (Lausanne), 2022. **13**: p. 910978.
649 25. Swaminathan, G., B. Varghese, and S.Y. Fuchs, *Regulation of prolactin receptor levels and activity*
650 *in breast cancer.* J Mammary Gland Biol Neoplasia, 2008. **13**(1): p. 81-91.
651 26. Hachim, I.Y., et al., *Prolactin Receptor Expression is an Independent Favorable Prognostic Marker*
652 *in Human Breast Cancer.* Appl Immunohistochem Mol Morphol, 2016. **24**(4): p. 238-45.
653 27. Hachim, I.Y., et al., *A favorable role of prolactin in human breast cancer reveals novel pathway-*
654 *based gene signatures indicative of tumor differentiation and favorable patient outcome.* Hum
655 Pathol, 2016. **53**: p. 142-52.
656 28. Lopez-Ozuna, V.M., et al., *Prolactin Pro-Differentiation Pathway in Triple Negative Breast*
657 *Cancer: Impact on Prognosis and Potential Therapy.* Sci Rep, 2016. **6**: p. 30934.
658 29. Hachim, I.Y., et al., *Prolactin hormone exerts anti-tumorigenic effects in HER-2 overexpressing*
659 *breast cancer cells through regulation of stemness.* Stem Cell Res, 2019. **40**: p. 101538.
660 30. Agarwal, N., et al., *Phase I Study of the Prolactin Receptor Antagonist LFA102 in Metastatic*
661 *Breast and Castration-Resistant Prostate Cancer.* Oncologist, 2016. **21**(5): p. 535-6.
662 31. Huising, M.O., C.P. Kruiswijk, and G. Flik, *Phylogeny and evolution of class-I helical cytokines.* J
663 Endocrinol, 2006. **189**(1): p. 1-25.
664 32. Teilum, K., et al., *Solution structure of human prolactin.* J Mol Biol, 2005. **351**(4): p. 810-23.
665 33. Dehkhoda, F., et al., *The Growth Hormone Receptor: Mechanism of Receptor Activation, Cell*
666 *Signaling, and Physiological Aspects.* Front Endocrinol (Lausanne), 2018. **9**: p. 35.
667 34. Waters, M.J., *The growth hormone receptor.* Growth Horm IGF Res, 2016. **28**: p. 6-10.
668 35. Araya-Secchi, R., et al., *The prolactin receptor scaffolds Janus kinase 2 via co-structure formation*
669 *with phosphoinositide-4,5-bisphosphate.* Elife, 2023. **12**.
670 36. Ross, R.J., et al., *A short isoform of the human growth hormone receptor functions as a dominant*
671 *negative inhibitor of the full-length receptor and generates large amounts of binding protein.*
672 Mol Endocrinol, 1997. **11**(3): p. 265-73.
673 37. Kavarthapu, R. and M.L. Dufau, *Prolactin receptor gene transcriptional control, regulatory*
674 *modalities relevant to breast cancer resistance and invasiveness.* Front Endocrinol (Lausanne),
675 2022. **13**: p. 949396.
676 38. Biener-Ramanujan, E., et al., *Spatio-temporal kinetics of growth hormone receptor signaling in*
677 *single cells using FRET microscopy.* Growth Hormone & Igf Research, 2006. **16**(4): p. 247-257.
678 39. Brooks, A.J., et al., *Mechanism of activation of protein kinase JAK2 by the growth hormone*
679 *receptor.* Science, 2014. **344**(6185): p. 1249783.
680 40. Liu, Y., et al., *Dynamic analysis of GH receptor conformational changes by split luciferase*
681 *complementation.* Mol Endocrinol, 2014. **28**(11): p. 1807-19.
682 41. Cunningham, B.C., et al., *Zinc mediation of the binding of human growth hormone to the human*
683 *prolactin receptor.* Science, 1990. **250**(4988): p. 1709-12.
684 42. Kossiakoff, A.A., et al., *Comparison of the intermediate complexes of human growth hormone*
685 *bound to the human growth hormone and prolactin receptors.* Protein Sci, 1994. **3**(10): p. 1697-
686 705.
687 43. Fu, Y.K., et al., *Growth hormone augments superoxide anion secretion of human neutrophils by*
688 *binding to the prolactin receptor.* J Clin Invest, 1992. **89**(2): p. 451-7.
689 44. Somers, W., et al., *The X-ray structure of a growth hormone-prolactin receptor complex.* Nature,
690 1994. **372**(6505): p. 478-81.

691 45. Hughes, J.P. and H.G. Friesen, *The nature and regulation of the receptors for pituitary growth*
692 *hormone.* Annu Rev Physiol, 1985. **47**: p. 469-82.
693 46. Frank, S.J., *Classical and novel GH receptor signaling pathways.* Mol Cell Endocrinol, 2020. **518**:
694 p. 110999.
695 47. Chhabra, Y., et al., *GHR signalling: Receptor activation and degradation mechanisms.* Mol Cell
696 Endocrinol, 2021. **520**: p. 111075.
697 48. Argetsinger, L.S., et al., *Identification of JAK2 as a growth hormone receptor-associated tyrosine*
698 *kinase.* Cell, 1993. **74**(2): p. 237-44.
699 49. Smit, L.S., et al., *The role of the growth hormone (GH) receptor and JAK1 and JAK2 kinases in the*
700 *activation of Stats 1, 3, and 5 by GH.* Mol Endocrinol, 1996. **10**(5): p. 519-33.
701 50. Lebrun, J.J., et al., *Prolactin-induced proliferation of Nb2 cells involves tyrosine phosphorylation*
702 *of the prolactin receptor and its associated tyrosine kinase JAK2.* J Biol Chem, 1994. **269**(19): p.
703 14021-6.
704 51. DaSilva, L., et al., *Prolactin recruits STAT1, STAT3 and STAT5 independent of conserved receptor*
705 *tyrosines TYR402, TYR479, TYR515 and TYR580.* Mol Cell Endocrinol, 1996. **117**(2): p. 131-40.
706 52. Winston, L.A. and T. Hunter, *JAK2, Ras, and Raf are required for activation of extracellular signal-*
707 *regulated kinase/mitogen-activated protein kinase by growth hormone.* J Biol Chem, 1995.
708 **270**(52): p. 30837-40.
709 53. Abe, J. and B.C. Berk, *Fyn and JAK2 mediate Ras activation by reactive oxygen species.* J Biol
710 Chem, 1999. **274**(30): p. 21003-10.
711 54. Waters, M.J. and A.J. Brooks, *JAK2 activation by growth hormone and other cytokines.* Biochem
712 J, 2015. **466**(1): p. 1-11.
713 55. Vansaun, M.N., *Molecular pathways: adiponectin and leptin signaling in cancer.* Clin Cancer Res,
714 2013. **19**(8): p. 1926-32.
715 56. Platanias, L.C., *Mechanisms of type-I- and type-II-interferon-mediated signalling.* Nat Rev
716 Immunol, 2005. **5**(5): p. 375-86.
717 57. Bousoik, E. and H. Montazeri Aliabadi, *"Do We Know Jack" About JAK? A Closer Look at JAK/STAT*
718 *Signaling Pathway.* Front Oncol, 2018. **8**: p. 287.
719 58. Hu, X., et al., *The JAK/STAT signaling pathway: from bench to clinic.* Signal Transduct Target
720 Ther, 2021. **6**(1): p. 402.
721 59. Dawson, M.A., et al., *JAK2 phosphorylates histone H3Y41 and excludes HP1alpha from*
722 *chromatin.* Nature, 2009. **461**(7265): p. 819-22.
723 60. Seavey, M.M. and P. Dobrzanski, *The many faces of Janus kinase.* Biochem Pharmacol, 2012.
724 **83**(9): p. 1136-45.
725 61. Bridges, R.S. and D.R. Grattan, *30 years after: CNS actions of prolactin: Sources, mechanisms and*
726 *physiological significance.* J Neuroendocrinol, 2019. **31**(3): p. e12669.
727 62. Wen, Y., et al., *Blockade of the Short Form of Prolactin Receptor Induces FOXO3a/EIF-4EBP1-*
728 *Mediated Cell Death in Uterine Cancer.* Mol Cancer Ther, 2020. **19**(9): p. 1943-1954.
729 63. Molina-Salinas, G., et al., *Decoding signaling pathways involved in prolactin-induced*
730 *neuroprotection: A review.* Front Neuroendocrinol, 2021. **61**: p. 100913.
731 64. Carter-Su, C., J. Schwartz, and L.S. Argetsinger, *Growth hormone signaling pathways.* Growth
732 Horm IGF Res, 2016. **28**: p. 11-5.
733 65. Chasseloup, F., V. Bernard, and P. Chanson, *Prolactin: structure, receptors, and functions.* Rev
734 Endocr Metab Disord, 2024.
735 66. Herman, A., et al., *Functional heterodimerization of prolactin and growth hormone receptors by*
736 *ovine placental lactogen.* J Biol Chem, 2000. **275**(9): p. 6295-301.
737 67. Biener, E., et al., *Ovine placental lactogen-induced heterodimerization of ovine growth hormone*
738 *and prolactin receptors in living cells is demonstrated by fluorescence resonance energy transfer*

739 *microscopy and leads to prolonged phosphorylation of signal transducer and activator of*
740 *transcription (STAT)1 and STAT3.* Endocrinology, 2003. **144**(8): p. 3532-40.
741 68. Xu, J., et al., *Growth hormone signaling in human T47D breast cancer cells: potential role for a*
742 *growth hormone receptor-prolactin receptor complex.* Mol Endocrinol, 2011. **25**(4): p. 597-610.
743 69. Liu, Y., et al., *GHR/PRLR Heteromultimer Is Composed of GHR Homodimers and PRLR*
744 *Homodimers.* Mol Endocrinol, 2016. **30**(5): p. 504-17.
745 70. Liu, Y., et al., *Subdomain 2, Not the Transmembrane Domain, Determines the Dimerization*
746 *Partner of Growth Hormone Receptor and Prolactin Receptor.* Endocrinology, 2017. **158**(10): p.
747 3235-3248.
748 71. Huang, B., H. Babcock, and X. Zhuang, *Breaking the diffraction barrier: super-resolution imaging*
749 *of cells.* Cell, 2010. **143**(7): p. 1047-58.
750 72. Bates, M., T.R. Blosser, and X. Zhuang, *Short-range spectroscopic ruler based on a single-*
751 *molecule optical switch.* Phys Rev Lett, 2005. **94**(10): p. 108101.
752 73. Kruger, C.L., et al., *Quantitative single-molecule imaging of TLR4 reveals ligand-specific receptor*
753 *dimerization.* Sci Signal, 2017. **10**(503).
754 74. Krüger, C., et al., *Molecular counting of membrane receptor subunits with single-molecule*
755 *localization microscopy*. SPIE BiOS. Vol. 10071. 2017: SPIE.
756 75. Ripley, B.D., *Tests of `Randomness' for Spatial Point Patterns.* Journal of the Royal Statistical
757 Society. Series B (Methodological), 1979. **41**(3): p. 368-374.
758 76. Ester, M., et al., *A density-based algorithm for discovering clusters in large spatial databases*
759 *with noise*, in *Proceedings of the Second International Conference on Knowledge Discovery and*
760 *Data Mining*. 1996, AAAI Press: Portland, Oregon. p. 226–231.
761 77. Mattheyses, A.L., S.M. Simon, and J.Z. Rappoport, *Imaging with total internal reflection*
762 *fluorescence microscopy for the cell biologist.* J Cell Sci, 2010. **123**(Pt 21): p. 3621-8.
763 78. Kohlhuber, F., et al., *A JAK1/JAK2 chimera can sustain alpha and gamma interferon responses.*
764 Mol Cell Biol, 1997. **17**(2): p. 695-706.
765 79. Loesch, K., et al., *Janus kinase 2 influences growth hormone receptor metalloproteolysis.*
766 Endocrinology, 2006. **147**(6): p. 2839-49.
767 80. Deng, L., et al., *Determinants of growth hormone receptor down-regulation.* Mol Endocrinol,
768 2007. **21**(7): p. 1537-51.
769 81. Zhang, Y., et al., *Growth hormone (GH) receptor (GHR)-specific inhibition of GH-Induced signaling*
770 *by soluble IGF-1 receptor (sol IGF-1R).* Mol Cell Endocrinol, 2019. **492**: p. 110445.
771 82. Zhang, Y., et al., *Growth hormone (GH)-induced dimerization inhibits phorbol ester-stimulated*
772 *GH receptor proteolysis.* J Biol Chem, 2001. **276**(27): p. 24565-73.
773 83. Chen, H., et al., *Augmented Stat5 Signaling Bypasses Multiple Impediments to Lactogen-*
774 *Mediated Proliferation in Human beta-Cells.* Diabetes, 2015. **64**(11): p. 3784-97.
775 84. Jiang, J., et al., *A conformationally sensitive GHR [growth hormone (GH) receptor] antibody:*
776 *impact on GH signaling and GHR proteolysis.* Mol Endocrinol, 2004. **18**(12): p. 2981-96.
777 85. Kim, S.O., et al., *Involvement of the Src homology 2-containing tyrosine phosphatase SHP-2 in*
778 *growth hormone signaling.* J Biol Chem, 1998. **273**(4): p. 2344-54.
779 86. Zhang, Y., et al., *Disulfide linkage of growth hormone (GH) receptors (GHR) reflects GH-induced*
780 *GHR dimerization. Association of JAK2 with the GHR is enhanced by receptor dimerization.* J Biol
781 Chem, 1999. **274**(46): p. 33072-84.
782 87. Alele, J., et al., *Blockade of growth hormone receptor shedding by a metalloprotease inhibitor.*
783 Endocrinology, 1998. **139**(4): p. 1927-35.
784 88. Frank, S.J., et al., *In vivo imaging of hepatic growth hormone signaling.* Mol Endocrinol, 2006.
785 **20**(11): p. 2819-30.

786 89. He, K., et al., *Janus kinase 2 enhances the stability of the mature growth hormone receptor.*
787 Endocrinology, 2005. **146**(11): p. 4755-65.
788 90. Yang, N., et al., *Role of the growth hormone (GH) receptor transmembrane domain in receptor*
789 *predimerization and GH-induced activation.* Mol Endocrinol, 2007. **21**(7): p. 1642-55.
790 91. Yang, N., et al., *Activation of growth hormone receptors by growth hormone and growth*
791 *hormone antagonist dimers: insights into receptor triggering.* Mol Endocrinol, 2008. **22**(4): p.
792 978-88.
793 92. Gan, Y., et al., *Human GH receptor-IGF-1 receptor interaction: implications for GH signaling.* Mol
794 Endocrinol, 2014. **28**(11): p. 1841-54.
795 93. Buckels, A., et al., *Autocrine/paracrine actions of growth hormone in human melanoma cell lines.*
796 Biochem Biophys Rep, 2020. **21**: p. 100716.
797 94. Beggs, R.R., W.F. Dean, and A.L. Mattheyses, *dSTORM Imaging and Analysis of Desmosome*
798 *Architecture*, in *Permeability Barrier: Methods and Protocols*, K. Turksen, Editor. 2021, Springer
799 US: New York, NY. p. 305-315.
800 95. Beggs, R.R., W.F. Dean, and A.L. Mattheyses, *dSTORM Imaging and Analysis of Desmosome*
801 *Architecture.* Methods Mol Biol, 2020.
802 96. Beggs, R.R., et al., *Desmosomes undergo dynamic architectural changes during assembly and*
803 *maturation.* Tissue Barriers, 2022. **10**(4): p. 2017225.
804 97. Pageon, S.V., et al., *Clus-DoC: a combined cluster detection and colocalization analysis for single-*
805 *molecule localization microscopy data.* Mol Biol Cell, 2016. **27**(22): p. 3627-3636.
806 98. Ran, F.A., et al., *Double nicking by RNA-guided CRISPR Cas9 for enhanced genome editing*
807 *specificity.* Cell, 2013. **154**(6): p. 1380-9.
808 99. Ran, F.A., et al., *Genome engineering using the CRISPR-Cas9 system.* Nat Protoc, 2013. **8**(11): p.
809 2281-2308.
810 100. Zhou, Y., et al., *A mammalian model for Laron syndrome produced by targeted disruption of the*
811 *mouse growth hormone receptor/binding protein gene (the Laron mouse).* Proc Natl Acad Sci U S
812 A, 1997. **94**(24): p. 13215-20.
813 101. Frank, S.J., *Receptor dimerization in GH and erythropoietin action--it takes two to tango, but*
814 *how?* Endocrinology, 2002. **143**(1): p. 2-10.
815 102. Cunningham, B.C., et al., *Dimerization of the extracellular domain of the human growth hormone*
816 *receptor by a single hormone molecule.* Science, 1991. **254**(5033): p. 821-5.
817 103. Gent, J., et al., *Ligand-independent growth hormone receptor dimerization occurs in the*
818 *endoplasmic reticulum and is required for ubiquitin system-dependent endocytosis.* Proc Natl
819 Acad Sci U S A, 2002. **99**(15): p. 9858-63.
820 104. Gadd, S.L. and C.V. Clevenger, *Ligand-independent dimerization of the human prolactin receptor*
821 *isoforms: functional implications.* Mol Endocrinol, 2006. **20**(11): p. 2734-46.
822 105. Wilmes, S., et al., *Mechanism of homodimeric cytokine receptor activation and dysregulation by*
823 *oncogenic mutations.* Science, 2020. **367**(6478): p. 643-652.
824 106. Pezet, A., et al., *The last proline of Box 1 is essential for association with JAK2 and functional*
825 *activation of the prolactin receptor.* Mol Cell Endocrinol, 1997. **129**(2): p. 199-208.
826 107. Kassem, N., et al., *Order and disorder-An integrative structure of the full-length human growth*
827 *hormone receptor.* Sci Adv, 2021. **7**(27).
828 108. Bugge, K., et al., *A combined computational and structural model of the full-length human*
829 *prolactin receptor.* Nat Commun, 2016. **7**: p. 11578.
830 109. Ferrao, R.D., H.J. Wallweber, and P.J. Lupardus, *Receptor-mediated dimerization of JAK2 FERM*
831 *domains is required for JAK2 activation.* Elife, 2018. **7**.
832 110. Neville, M.C., T.B. McFadden, and I. Forsyth, *Hormonal regulation of mammary differentiation*
833 *and milk secretion.* J Mammary Gland Biol Neoplasia, 2002. **7**(1): p. 49-66.

111. Pirchio, R., et al., *Metabolic effects of prolactin.* Front Endocrinol (Lausanne), 2022. **13**: p. 1015520.
112. Macotela, Y., J. Triebel, and C. Clapp, *Time for a New Perspective on Prolactin in Metabolism.* Trends Endocrinol Metab, 2020. **31**(4): p. 276-286.
113. Vijayakumar, A., S. Yakar, and D. Leroith, *The intricate role of growth hormone in metabolism.* Front Endocrinol (Lausanne), 2011. **2**: p. 32.
114. Lu, J.C., T.M. Piazza, and L.A. Schuler, *Proteasomes mediate prolactin-induced receptor down-regulation and fragment generation in breast cancer cells.* J Biol Chem, 2005. **280**(40): p. 33909-16.
115. Chhabra, Y., et al., *Tyrosine kinases compete for growth hormone receptor binding and regulate receptor mobility and degradation.* Cell Rep, 2023. **42**(5): p. 112490.
116. Yonezawa, T., et al., *Anti-metastatic outcome of isoform-specific prolactin receptor targeting in breast cancer.* Cancer Lett, 2015. **366**(1): p. 84-92.
117. Erika, G., et al., *Prolactin Receptor Isoforms in Human Breast Cancer*, in *Prolactin*, M.N. György and E.T. Bela, Editors. 2013, IntechOpen: Rijeka. p. Ch. 11.
118. Taghi Khani, A., et al., *Isoform-specific knockdown of long and intermediate prolactin receptors interferes with evolution of B-cell neoplasms.* Commun Biol, 2023. **6**(1): p. 295.